

Review article



Experimental in vitro, ex vivo and in vivo models in prostate cancer research

Verena Sailer¹, Gunhild von Amsberg², Stefan Duensing³, Jutta Kirfel¹, Verena Lieb⁴, Eric Metzger⁵, Anne Offermann¹, Klaus Pantel^{6,7}, Roland Schuele⁵, Helge Taubert⁴, Sven Wach⁴, Sven Perner^{8,9}, Stefan Werner^{6,7} & Achim Aigner¹⁰✉

Abstract

Androgen deprivation therapy has a central role in the treatment of advanced prostate cancer, often causing initial tumour remission before increasing independence from signal transduction mechanisms of the androgen receptor and then eventual disease progression. Novel treatment approaches are urgently needed, but only a fraction of promising drug candidates from the laboratory will eventually reach clinical approval, highlighting the demand for critical assessment of current preclinical models. Such models include standard, genetically modified and patient-derived cell lines, spheroid and organoid culture models, scaffold and hydrogel cultures, tissue slices, tumour xenograft models, patient-derived xenograft and circulating tumour cell eXplant models as well as transgenic and knockout mouse models. These models need to account for inter-patient and intra-patient heterogeneity, the acquisition of primary or secondary resistance, the interaction of tumour cells with their microenvironment, which make crucial contributions to tumour progression and resistance, as well as the effects of the 3D tissue network on drug penetration, bioavailability and efficacy.

Sections

Introduction

Cell lines as 2D in vitro models

3D models

Tumour xenograft models

Patient-derived xenografts

CTC eXplant models

Transgenic and genetically engineered mouse models

Sophisticated models meet sophisticated analytics

Translating success from models to clinics

Conclusions

¹Institute for Pathology, University Hospital Schleswig-Holstein, Campus Lübeck, Lübeck, Germany. ²Department of Oncology and Hematology, University Cancer Center Hamburg Eppendorf and Martini-Klinik, Prostate Cancer Center, University Hospital Hamburg Eppendorf, Hamburg, Germany. ³Section of Molecular Urooncology, Department of Urology, University Hospital Heidelberg and National Center for Tumour Diseases, Heidelberg, Germany. ⁴Research Division Molecular Urology, Department of Urology and Paediatric Urology, University Hospital Erlangen, Erlangen, Germany. ⁵Department of Urology, Center for Clinical Research, University of Freiburg Medical Center, Freiburg, Germany. ⁶Institute for Tumour Biology, Center for Experimental Medicine, University Clinics Hamburg-Eppendorf, Hamburg, Germany. ⁷Mildred-Scheel-Nachwuchszentrum HaTRiCs4, University Cancer Center Hamburg, Hamburg, Germany. ⁸University Hospital Schleswig-Holstein, Campus Lübeck, Lübeck, Germany. ⁹Pathology, Research Center Borstel, Leibniz Lung Center, Borstel, Germany. ¹⁰Clinical Pharmacology, Rudolf-Boehm-Institute for Pharmacology and Toxicology, University of Leipzig, Medical Faculty, Leipzig, Germany. ✉e-mail: achim.aigner@medizin.uni-leipzig.de

Review article

Key points

- Ideally, tumour models will reflect inter-patient and intra-patient heterogeneity, primary and/or secondary resistance, the interaction of tumour cells with their microenvironment, and the effects of the 3D tissue architecture on drug penetration, bioavailability and efficacy.
- Various in vitro, ex vivo and in vivo models exist, each associated with defined advantages and disadvantages.
- In vitro and ex vivo models include standard, genetically modified and patient-derived cell lines, spheroid and organoid culture models, scaffold and hydrogel cultures, and tissue slice models.
- In vivo models — including tumour xenografts, patient-derived xenografts and circulating tumour cell eXplant models, as well as transgenic and knockout mouse models — are still indispensable for prostate cancer research.
- Successful experimental prostate cancer research will require exploration of the full complexity of the disease, relying on the combined use of the broad spectrum of models.
- Novel approaches will be required for holistic and sophisticated analyses, for example, characterizations at a single-cell level in vivo or the extensive integration of computational and/or artificial intelligence-based approaches.

Introduction

Prostate cancer is the most common malignancy and second leading cause of cancer-related death amongst men in the Western world¹. Approximately 80% of men are diagnosed with organ-confined disease, 15% with locoregional metastases and 5% with distant metastases² and life expectancy for men with localized disease can be as high as 99% over 10 years³. By contrast, the prognosis of men with advanced disease remains variable, with most men eventually succumbing to the disease — men who are diagnosed with metastatic disease have a poor overall survival of only 30% at 5 years³. Considerable treatment success has been achieved over the past two decades for patients with advanced or metastatic disease and survival benefit has been demonstrated for drugs with different efficacy profiles in several landmark phase III clinical trials, such as androgen receptor (AR) or AR pathway-targeting drugs (abiraterone in combination with prednisone, enzalutamide, apalutamide and darolutamide), as well as classical chemotherapeutic agents (docetaxel and cabazitaxel), radionuclides (radium-223) and immunotherapeutics (sipuleucel T)⁴. In addition, poly(ADP-ribose) polymerase (PARP) inhibitors are now available for patients harbouring mutations resulting in deficient homologous recombination repair (HRR)⁵, and PSMA radioligand therapy has demonstrated a prolonged overall survival benefit compared with standard of care alone⁶. Of note, therapies initially developed for late-stage disease (metastatic castration-resistant prostate cancer; mCRPC) have been integrated earlier in the treatment portfolio with new standards of care for metastatic hormone-naïve prostate cancer and non-metastatic CRPC⁷. Nevertheless, despite this progress, development of resistance and aggressive variants of disease remain a major therapeutic challenge.

Prostate cancer is characterized by its heterogeneity, with multiple tumour foci often being present synchronously in the same organ⁸.

Various factors contribute towards this heterogeneity, including underlying cancer-driving genomic alterations, zonal anatomy, tumour growth patterns that are recognized in the various patterns of the Gleason grading, and treatment-related alterations (Fig. 1). The Gleason grading system is applied to assess and classify histological features of tumour architecture. Different compartments are interlinked; for example, driver events and zonal anatomy⁸. The underlying reasons for this interplay are ill-understood and challenging to model. In advanced and metastatic stages, molecular heterogeneity is decreased in the individual patient, but spatial distribution of metastases and predilection for anatomical sites such as bone occur, and inter-patient heterogeneity becomes more common⁹.

Underlying cancer-driving molecular alterations include chromosomal events and mutations, as well as epigenetic changes. Most primary prostate tumours are molecularly defined by one of seven subtypes¹⁰. The most common chromosomal alteration is the gene fusion of ETS transcription factors ERG and ETV1 with TMPRSS2 (ref.¹¹). This event highlights the complex nature of multifocal disease, as different chromosomal changes can be found in what morphologically seems to be the same tumour nodule^{12,13}. In almost two-thirds of patients, multiple genetically distinct subclones are found¹⁴. Further driver events, such as recurrent mutations in SPOP or FOXA1, epigenetic alterations and alterations in targetable pathways such as DNA repair and PI3K signalling, as well as differentially expressed genes, highlight the genomic heterogeneity of prostate cancer¹⁵.

Zonal anatomy has a pivotal role in development and progression of prostate cancer. Cancer arising in the transition zone is associated with more favourable outcomes than cancer that arises at the periphery of the gland. The molecular make-up of the tumour is characterized by driver alterations that are enriched according to the respective zone. For instance, TMPRSS2–ERG fusions are much more prevalent in peripheral zone tumours than in transition zone tumours¹⁶.

Gleason grading is based solely on architectural features and is one of the most powerful prognosticators of the course of the disease. Often, several tumour nodules within one prostate display distinctly heterogeneous growth patterns, that is, Gleason patterns. Different groups, such as the International Society of Urological Pathology and the Genitourinary Pathology Society, have tried to find a consensus regarding how to grade different tumour nodules in radical prostatectomy samples¹⁷. On the molecular level, an increased Gleason score or grade group positively correlates with a genotype complexity¹⁸. Even within the morphologically defined group of high-grade prostate cancers, those tumours displaying increased genomic diversity tend to demonstrate a reduced response to neoadjuvant androgen deprivation therapy (ADT)¹⁹.

Treatment-related changes mostly apply to the genomic landscape of pretreated advanced or metastatic disease; therefore, they are more relevant in the late stages of prostate cancer. For instance, amplification, pathogenic mutations or splice variants of the AR are present in up to 85% of men with CRPC, suggesting the presence of an escape strategy following selective pressure under ADT and AR targeting agents. Another resistance mechanism is treatment-associated transdifferentiation with emergence of a completely AR-independent small-cell phenotype²⁰. Overall, the genomic landscape of metastatic disease differs substantially from that of primary prostate cancer²¹.

All these compartments in which heterogeneity can occur are challenging to model. For a comprehensive understanding of prostate cancer, the different preclinical models can be viewed as layers, whereby each layer contributes one or several pieces of information that,

taken together, can elucidate prostate carcinogenesis and ultimately contribute to improved patient care.

The tumour microenvironment (TME) also has an important role in understanding cancer progression and metastatic spread in prostate cancer. The TME consists of stromal cells, the vascular compartment and immune cells²². The most prevalent anatomical site of prostate cancer metastases is bone and the interplay between prostate cancer cells and the bony metastatic niche has been explored over the past few years²³. Immune cells in particular have come into focus as targets of immunotherapeutic agents, such as immune checkpoint inhibitors (ICIs), which have revolutionized treatment for cancer types such as non-small-cell lung cancer and melanoma^{24,25}. However, prostate cancer is regarded as a ‘cold’ tumour that does not have the propensity to generate an adequate antitumour immune response. Thus, ICIs

have demonstrated only limited therapeutic benefit for a subset of patients with prostate cancer²⁶. Given the importance of the TME and the immune environment, any preclinical model that addresses metastasis formation must take TME components into account.

In this Review, we provide a comprehensive overview of various *in vitro*, *ex vivo* and *in vivo* models and discuss their respective advantages and limitations in the context of current needs and challenges in prostate cancer research and therapy.

Cell lines as 2D *in vitro* models

Despite some shortcomings, prostate cancer cell lines in conventional 2D monolayer culture still provide valuable and frequently used *in vitro* systems for studying cellular and molecular mechanisms, as well as drug effects, without the limitations of primary tissue availability or

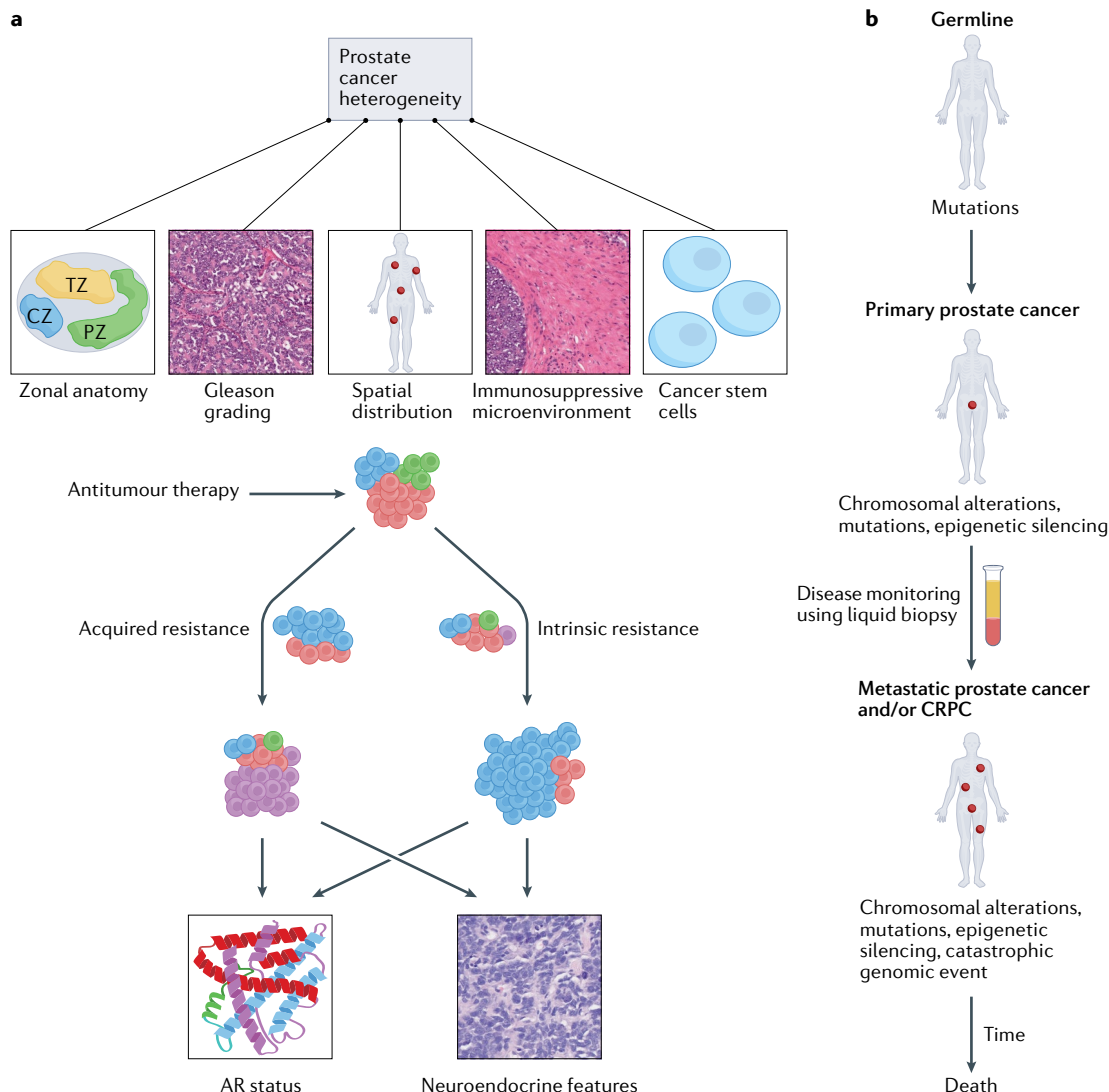


Fig. 1 | Cellular properties and molecular hallmarks of prostate cancer.

a, A plethora of characteristics contribute to prostate cancer heterogeneity. These include zonal anatomy, tumour grading, spatial distribution of metastases and the respective organ-specific microenvironment as well as multiple tumour foci arising from different cancer stem cells. In the event of metastatic disease and subsequent application of treatment, subclones emerge, which show

either acquired or de novo resistance. Neuroendocrine transdifferentiation in particular poses a diagnostic as well as a therapeutic challenge and is also difficult to model. **b**, The disease course of prostate cancer progresses with an accumulation of molecular events over time, some of which are amenable to monitoring via liquid biopsy. AR, androgen receptor; CRPC, castration-resistant prostate cancer; CZ, central zone; PZ, peripheral zone; TZ, transition zone.

insufficient cell numbers. Also, cell lines provide an unlimited source of cells for generating xenotransplant or orthotopic animal *in vivo* models^{27–30}.

Genetic profiling of prostate cancer cell lines has revealed relatively high genomic stability of cancer cell lines over the years²⁷. Importantly, cell line models must faithfully recapitulate the natural course of the disease from hormone sensitivity to the different levels of hormone independence, mediated by the various mechanisms of drug resistance, and the development of metastases. Prostate cancer cell lines can originate from prostate cancer tissue (primary tumour or metastases), from xenotransplanted isolated tumour cells or from patient-derived xenografts (PDXs)³⁰. However, the establishment of stable cell lines or even long-term PDX models remains a challenging task. For instance, the establishment of the LuCaP series has been ongoing since 1996, with 251 individual PDXs having been attempted from 156 patients. Of these, only 21 long-term PDXs have emerged that were stable for three passages³¹. Attempts to transfer the LuCaP models into a stable 2D monolayer culture were unsuccessful³². In addition to the three mainly used ‘classical’ prostate cancer cell lines – DU145 (ref.³³), PC-3 (ref.³⁴) and LNCaP³⁵ – more than 35 prostate cancer cell lines have been established, but several of them originate from these three cell lines^{27,28,30} (Table 1 and Supplementary Tables 1 and 2).

Prostate cancer cell lines can be classified by different characteristics, including their site of origin, xenotransplant passage (if applicable), histopathology and androgen dependency status. In addition, short tandem repeat profiling is important to verify their origin and to exclude contamination by cells from another tumour entity (for example, HeLa cells), other prostate cancer cells (yielding a prostate cancer cell mixture) or somatic cells (such as tumour-associated fibroblasts). Examples of prostate cancer cell line misclassification are the cell lines ALVA-31, ALVA-41 and DuPro-1, which, based on karyotypic characterization or DNA profiling analysis, have been identified as clonal derivatives of PC-3 cells^{27,36}. In addition, DNA profiles of MDA PCa 1 and ARCaP are identical. The same applies for the two prostate cancer cell lines DuCaP and VCaP. Furthermore, MDA PCa 2a and MDA PCa 2b have very similar DNA profiles, strongly supporting the notion of a common origin²⁷. The characterization of cell lines can even identify a different tumour entity as the origin; for example, the cell line TSU-Pr1, which was originally thought to be derived from prostate cancer, was subsequently characterized as being derived from bladder cancer^{27,37}.

Only a few cell lines – 1013 L, UM-SCP-1, PSK-1 and PPC-1 – originate from primary tumours, and most of the current cell lines including the so-called classical cell lines, were derived from PCa metastases. For example, LNCaP, NCI-H660, ALVA-55 and LAPC-4 from lymph node metastases; DU145 from brain metastases; PC-3, ALVA-41, ALVA-101, MDA PCa 2a and MDA PCa 2b from bone metastases; and KuCaP13 from a penile metastasis. The DuPro, PC346C, 22Rv1 and LAPC-3 cell lines were obtained from PDX models originating from a primary tumour, whereas cell lines have also been generated from PDX originating from metastases of lymph nodes (LAP-C4), spinal cord (VCaP) or dura (DuCaP). The VCaP and DuCaP cell lines originate from distinct metastases from the same patient^{38–40}. Interestingly, VCaP cell lines can emit the Bxv-1 virus, which means that thorough safety protocols are required when working with VCaP cells⁴¹.

Histopathologically, most prostate tumours (about 95%) are acinar adenocarcinoma, a histological subtype derived from acinar cells or acinar ducts⁴². However, a small percentage are other rare histological subtypes, such as ductal adenocarcinoma (3%), squamous cell carcinoma (<0.6%) or neuroendocrine carcinoma (<2%)^{43,44}. Only one cell

line each has been described as originating from squamous cell cancer (UM-SCP-1), small cell carcinoma (PSK-1) or a neuroendocrine penile metastasis (KuCaP13) of a prostate tumour^{45–47}.

Prostate cancer cell lines can be mainly differentiated into three groups in terms of androgen dependency. Androgen-dependent (AD) cell lines require androgens for their growth; cells that are androgen-independent but androgen-sensitive (AI/AS), whereby androgens are not required for growth, but the cells show a growth response to androgens; and androgen-independent (AI) cell lines, for which androgen is neither needed nor affects growth²⁷. The only exception is the cell line ARCaP, in which growth is repressed by androgens²⁷. The classical AD cell line is LNCaP, but the cell lines PC346C and LAP-C4 also belong to this group. An increased number of cell lines are found in the AI/AS group, including MDA PCa 2a, MDA PCa 2b, 22Rv1, VCaP, DuCaP and CWR-R1. The AI group includes the other two classical prostate cancer cell lines, PC-3 and DU145, but also the cell lines 1013 L, UM-SCP-1, NCI-H660, MDA PCa 1, PSK-1, as well as the LNCaP derivatives LNCaP-C4 and LNCaP-C4-2. In most cases, AD or AI/AS behaviour coincides with the expression of the AR on the mRNA and protein level (Supplementary Table 1), whereas AI cells show no or only very weak AR expression. Somewhat intermediate is the cell line LNCaP-C4-2, which is AI despite some AR mRNA expression. AR alterations have a central role in disease progression and development of drug resistance and changes in AR are seen in >70% of patients with mCRPC. Thus, AR alterations are important considerations in prostate cancer cell lines. For example, the H875Y or T878A point mutations result in an antagonist-to-agonist switch and receptor promiscuity in patients with prostate cancer⁴⁸. These mutations are also found in prostate cancer cell lines, for example, H875Y (22Rv1, CWR-R1) and T878A (LNCaP, MDA PCa 2a and MDA-PCa 2b) (Supplementary Table 1). Androgen signalling also affects DNA damage signalling by differentially regulating a subset of DNA repair genes⁴⁹, and patients with alterations in HRR genes respond to PARP inhibitors; olaparib is approved for HRR gene-mutated mCRPC⁵⁰. Another frequently affected gene in mCRPC is the tumour suppressor gene TP53, with aberrations occurring in >50% of patients²¹. TP53 mutations can have a major role in therapy response in prostate cancer⁵¹, and this role and mutational status should be kept in mind when choosing appropriate prostate cancer cell lines for *in vitro* and *in vivo* studies (Supplementary Table 2). Notably, TP53-mutant proteins can be associated with increased subcutaneous tumour take rates in NOD-SCID mice⁵². Finally, so-called normal prostate cell lines are immortal cell lines formed either spontaneously or by manipulation. The latter refers to the infection or transfection with the Simian virus 40 (SV40) large T antigen gene, human papilloma virus (for example, HPV-16 or HPV-18), human telomerase reverse transcriptase or v-Ki-ras (Table 1).

In 2016, a transformed prostate cell line with features of neuroendocrine prostate cancer was established by purifying basal epithelial cells based on high protein expression of TROP2 and CD49. Enforced expression of MYC and activated AKT1 were then achieved using lentiviral transduction. *In vitro* propagation of these MYC–myrAKT1 tumour cells led to the establishment of a cell line named LASCPC-01, which grows rapidly in suspension and bears neuroendocrine and cancer stem cell-like features⁵³.

3D models

Several 3D culture systems have been developed for improved recapitulation of *in vivo* tissue organization and the TME, and aim to provide powerful platforms for analysing tumorigenesis and drug response without the need for *in vivo* experiments (Fig. 2). This aspect is important when considering the 3R principles (replace, reduce, refine) as a

Review article

Table 1 | ‘Normal’ prostate and prostate cancer cell lines^{27,28,30}

Cell line	Origin and characteristics	ATCC and/or source	Refs.
DU 145	Brain metastasis origin	ATCC (HTB-81)	33,189
1013L	Primary prostate tumour origin A rare non-acinar subtype of prostate carcinoma	Anita Bilström (Active Biotech Research AB, Lund, Sweden)	27,190,191
PC-3	Bone (lumbar) metastasis origin	ATCC (CRL-1435)	34
LNCaP	Lymph node metastasis origin	Julius Horoszewicz (Roswell Park Memorial Institute, Buffalo, NY, USA)	35,192
PC-93	Primary prostate cancer origin Seemed to contain HeLa cells	Gert Jan van Steenbrugge (Erasmus University, Rotterdam, Netherlands)	27,193,194
UM-SCP-1	Primary squamous cell carcinoma origin	Herb Barton Grossman (University of Texas, Houston, TX, USA)	45
NCI-H660	Lymph node metastasis extrapulmonary small cell carcinoma originating in the prostate gland origin	ATCC (CRL-5813)	195,196
DuPro-1	Primary, xenograft origin Very similar to PC-3 cells, according to karyotyping and DNA profiling	William Isaacs (Johns Hopkins University, Baltimore, MA, USA)	27,197
ALVA-101	Bone metastasis origin Very similar to PC-3 cells according to DNA profiling	Steven Loop (American Lake Veterans Administration Hospital, Tacoma, WA, USA)	27,198
ALVA-55	Lymph node metastasis origin Very similar to PC-3 cells, according to DNA profiling	Steven Loop (American Lake Veterans Administration Hospital, Tacoma, WA, USA)	27,199
PC-346C	Xenograft from primary prostate tumour	Wytse van Weerden (Erasmus University, Rotterdam, Netherlands)	129,200
ARCaP ^a	Ascites from patient with metastatic disease origin	Haiyen Zhai (University of Virginia, Charlottesville, VA, USA)	201
MDA PCa 1 ^a	Ascites origin	Nora Navone (University of Texas, Houston, TX, USA)	
LAPC-4	Xenograft established from lymph node metastasis	Charles Sawyer (University of California, Los Angeles, CA, USA)	202
MDA PCa 2a ^b	Bone metastasis origin (from the same African American male as MDA PCa 2b)	Nora Navone (University of Texas, Houston, TX, USA)	203,204
MDA PCa 2b ^b	Bone metastasis origin	ATCC (CRL-2422), Nora Navone (University of Texas, Houston, TX, USA)	203,204
CWR22	Xenograft model derived from a primary human prostatic carcinoma	NCI Division of Cancer Treatment and Diagnosis (DCTD) Tumour Repository	205,206
22Rv1 (CWR22Rv1)	Primary, xenograft derived from CWR22(R-2152)	ATCC (CRL-2505) James Jacobberger (Case Western Reserve University, Cleveland, OH, USA)	207
PSK-1	Primary squamous cell carcinoma origin	Chol Jang Kim (Shiga University of Medical Science, Otsu, Japan)	46
VCaP ^c	Xenograft derived from spinal cord metastasis Can emit Bxv-1 virus, thus requiring improved safety standards	ATCC (CRL-2876) Kenneth Pienta (University of Michigan, Ann Arbor, MI, USA)	38,40
DuCaP ^c	Xenograft derived from dura metastasis	Kenneth Pienta (University of Michigan, Ann Arbor, MI, USA)	38,39
CWR-R1	Primary xenograft from CWR22Rc cells	Christopher Gregory (University of North Carolina, Chapel Hill, NC, USA)	208
LNCaP-FGC	Clonal derivative of LNCaP cells	ATCC (CRL-1740)	35,192
LNCaP-LN-3	Metastatic subline of LNCaP cells derived by orthotopic implantation	Korean Cell Line Bank 80018	121
LNCaP-C4	Metastatic subline of LNCaP, derived after co-inoculation of LNCaP cells and fibroblasts	ATCC (CRL-3313)	120,209
LNCaP-C4-2	Metastatic sub-line derived from LNCaP-C4 cells after re-inoculation into castrated mice	ATCC (CRL-3315)	120,209
ALVA-31	Well-differentiated adenocarcinoma origin Might be derived from PC-3 cells, according to DNA profiling	No authentic stock is known	27,36,210
ALVA-41	Bone metastasis origin Might be derived from PC-3 cells, according to DNA profiling	No authentic stock is known	27,36,198,211
PPC-1	Poorly differentiated adenocarcinoma origin	No authentic stock is known	212
LAPC-3	Derived from a xenograft established from a TURP specimen	No authentic stock is known	202

Review article

Table 1 (continued) | ‘Normal’ prostate and prostate cancer cell lines^{27,28,30}

Cell line	Origin and characteristics	ATCC and/or source	Refs.
KuCaP13	Xenograft tumour from metastasis Characterized as neuroendocrine	No authentic stock is known	⁴⁷
LASCPC-01	MYC–myrAKT1 transduced cell line Neuroendocrine and cancer-stem cell-like features	ATCC (CRL-3356) Owen N. Witte (University of California, Los Angeles, CA, USA)	⁵³
P69SV40T	Immortalized cell line derived by transfection of adult prostate epithelial cells with the SV40 large T antigen gene	No authentic stock is known	²¹³
RWPE-2	Immortalized cell line initially derived by transfection of adult prostatic epithelial cells with HPV18, then made tumorigenic by infection with v-K-ras	ATCC (CRL-11610)	²¹⁴
CA-HPV-10	Immortalized cell line derived by HPV18 transfection of prostatic epithelial cells from a high-grade adenocarcinoma	ATCC (CRL-2220)	²¹⁵
PZ-HPV-7	Immortalized cell line derived by HPV18 transfection of normal prostatic peripheral zone epithelial cells	ATCC (CRL-2221)	²¹⁵
PWR-1E	Non-neoplastic, adult human prostate infected with the Ad12-SV40 virus	ATCC (CRL-11611)	²¹⁶
WPMY-1 normal prostatic myofibroblasts	SV40 large-T antigen-immortalized stromal cell line	ATCC (CRL-2854)	²¹⁷
E006AA	Spontaneously immortalized cells from an African American patient with a clinically localized prostate cancer	Walter Rayford (Louisiana State University-Health Sciences Center, New Orleans, LA, USA)	²¹⁸
hTERT EP156T	hTERT immortalized prostate primary epithelial cell line	ATCC (CRL-3289)	²¹⁹
RC-77T/E	HPV-16E6E7 immortalized primary prostate cancer cells of an American African patient	Clayton Yates (Tuskegee University, Tuskegee, AL, USA)	²²⁰
PNF-08	‘Normal’ prostate fibroblasts (not transformed)	Gerhard Unteregger (University of Saarland Medical School, Germany)	²²¹

See also Supplementary Tables 1 and 2 for additional information. Table 1 is an extended version based on the review articles of van Bokhoven et al.²⁷, Russell and Kingsley²⁸ and Namekawa et al.³⁰. HPV, human papilloma virus; hTERT, human telomerase reverse transcriptase; SV40, Simian virus 40; TURP, transurethral resection of the prostate. ^aMDA PCa 1 and ARCaP are derived from the same patient. ^bMDA PCa 2a and MDA PCa 2b are derived from the same patient. ^cVCaP and DuCaP are derived from the same patient.

road map for laboratory animal protection policies: to avoid animal experiments altogether (replacement), to limit the number of animals (reduction) and their suffering (refinement) in tests to an absolute minimum.

In general, 3D models can be categorized into either scaffold-free or scaffold-based systems. These groups include monocellular and multicellular tumour spheroids, cell-derived or tumour-derived spheroids, tumour-derived organoids, organotypic tissue slices, chorioallantoic membrane (CAM) models and tumour-on-a-chip systems.

3D models are aimed at more accurately monitoring the tumour’s in vivo features than 2D models, such as cell proliferation, differentiation, morphology, gene expression, signal transduction, metabolism, cell–cell interactions, tumour–stroma interactions and drug responses, all of which rely on the tumour cells’ microenvironment and, therefore, the tumour architecture⁵⁴. Various aspects of microenvironment and architecture, including intratumoural nutrient gradients, hypoxia, pH and/or acidosis and interstitial pressure, are inadequately represented in 2D culture⁵⁵. With regard to drug testing, tissue penetration and/or poor accessibility of the tumour cells in vivo can also be a concern. Development of 3D systems requires advances in the knowledge of tumour cell biology and microenvironment as well as novel technologies in microengineering and biofabrication. Microgravity can also affect growth and progression of prostate cancer cells^{56,57}. However, because of the absence of functional microvasculature, the in vivo situation can still be inadequately represented in some 3D models. In the drug testing field, another issue is the availability of powerful

readouts. Still, various 3D cell culture models are in use as in vitro tools for prostate cancer modelling and drug discovery⁵⁸.

Spheroid models

The formation of cell spheroids or tumour spheroids without matrix support can be performed using low-adhesion plates, by suspension cultures in appropriate devices for keeping the cells in suspension, or by the hanging-drop method (in which cells are placed in hanging-drop culture and incubated under physiological conditions⁵⁹), all of which result in cellular aggregation rather than their attachment onto a solid surface^{60,61}. The use of patient-derived material instead of immortalized cell lines can be particularly important from a translational viewpoint⁶²—despite immortalized cell lines retaining the driver mutations of the original tumour from which they were derived, alterations in the transcriptome indicate that the cellular characteristics have become adapted to cell culture rather than displaying the properties of the original primary tumour⁶³. In addition, spheroids exclusively generated from prostate cancer cell lines do not model tumour–stroma interactions, which are important in tumorigenesis and tumour growth. The applicability of spheroids in research also depends on their cultivation conditions⁵⁸. For example, although the hanging-drop technique enables use of small media volumes and cell numbers, subsequent media replacement is impossible and the precise addition of drugs is barely feasible. Overall, the use of spheroids in drug testing can be associated with issues, as no accurate drug response or cell viability assays have yet been developed⁵⁸.

In a 2010 study, a low-shear suspension culture model based on the spontaneous interaction of stromal and epithelial cells was described⁶⁴. As these structures contain both cell types with a tumour-tissue-like architecture, they were named ‘tumour histoids’⁶⁴. To create histoids, fibroblast spheroids were first generated, followed by the addition of PC3 cells. The process resulted in the generation of ~100 histoids in a 10-ml disposable culture chamber⁶⁴. In another study, a 3D multi-cell-type spheroid model was created to mimic metastatic prostate cancer. Here, a two-layer microfluidic system was used for the culture of fluorescently labelled metastatic prostate cancer cells (PC3 cell line), osteoblasts and endothelial cells, providing the tumour-cell-surrounding cell types in the bone microenvironment. A defined ratio of cells pre-mixed in a heterogeneous cell suspension ensured the uniform incorporation of all co-culture cell types into each spheroid. The lower proliferation rates of PC-3 cells without lowering viability resembled the *in vivo* growth behaviour of tumour cells within the bone metastatic prostate cancer microenvironment more closely than classical 2D culture⁶⁵.

Different prostate cancer cell lines and primary cells have been studied for their ability to form spheroids (which have also been termed ‘prostaspheres’ or ‘prostate spheres’) and patient-derived spheroids, respectively^{66,67}. In these studies, agarose-coated plates were used for measuring the prostasphere-forming potential of the cells, and single cells from established spheroids (at day 7) were further explored in secondary and tertiary spheroid assays. A CD49b^{hi}CD29^{hi}CD44^{hi} cell population was identified as being self-renewing tumour-initiating cells with particularly high potential for clonogenicity, tumorigenicity, migration and invasion, illustrating the way in which these *in vitro* models reflect the effects seen in *in vivo* models.

Studies of 3D spheroid suspension cultures generated from radical prostatectomy specimens demonstrated that the formation

of patient-derived spheroids is dependent on Gleason score, with a trend towards Gleason 6 or 7 being beneficial for spheroid formation, whereas Gleason 8–10 patterns were less efficient⁶⁸. Furthermore, large (>100 µm) spheroids often showed central necrosis, which is indicative of hypoxia; this necrosis was not seen in their smaller (40–100 µm) counterparts and indicates that spheroid size will affect its properties and homogeneity and/or heterogeneity, comparable with *in vivo* tumours. Spheroids could be successfully cryopreserved with little impairment of viability after thawing, enabling storage. Treatment of spheroids with bicalutamide or enzalutamide profoundly reduced cell viability, whereas treatment with docetaxel had very little effect and abiraterone had no effect at all⁶⁸. These differential effects are probably caused by the cells being derived from hormone-sensitive, organ-restricted primary tumours and were, therefore, characterized by a slow growth rate and not yet increased intratumoural androgen synthesis. However, cells from an established cell line (LNCaP) grown in 2D cell culture were also shown to be more sensitive, for example, to docetaxel, than their counterparts grown in spheroids⁶⁹. This characteristic further emphasizes the differences between results from 2D and 3D culture models, with 2D cell culture rather overestimating drug sensitivities.

Organoids

Patient-derived organoids (PDOs) for prostate cancer have also been established^{70,71}. Organoids in general can be developed either from healthy human or murine prostate tissues as well as from primary prostate tumours or metastatic lesions⁷². As tumour organoids, PDOs retain the molecular alterations – including AR signalling – present in the patient’s tumour, making organoids an excellent model for personalized *in vitro* research⁷³. This characteristic is particularly important in light of the complex molecular alterations that arise owing to selective

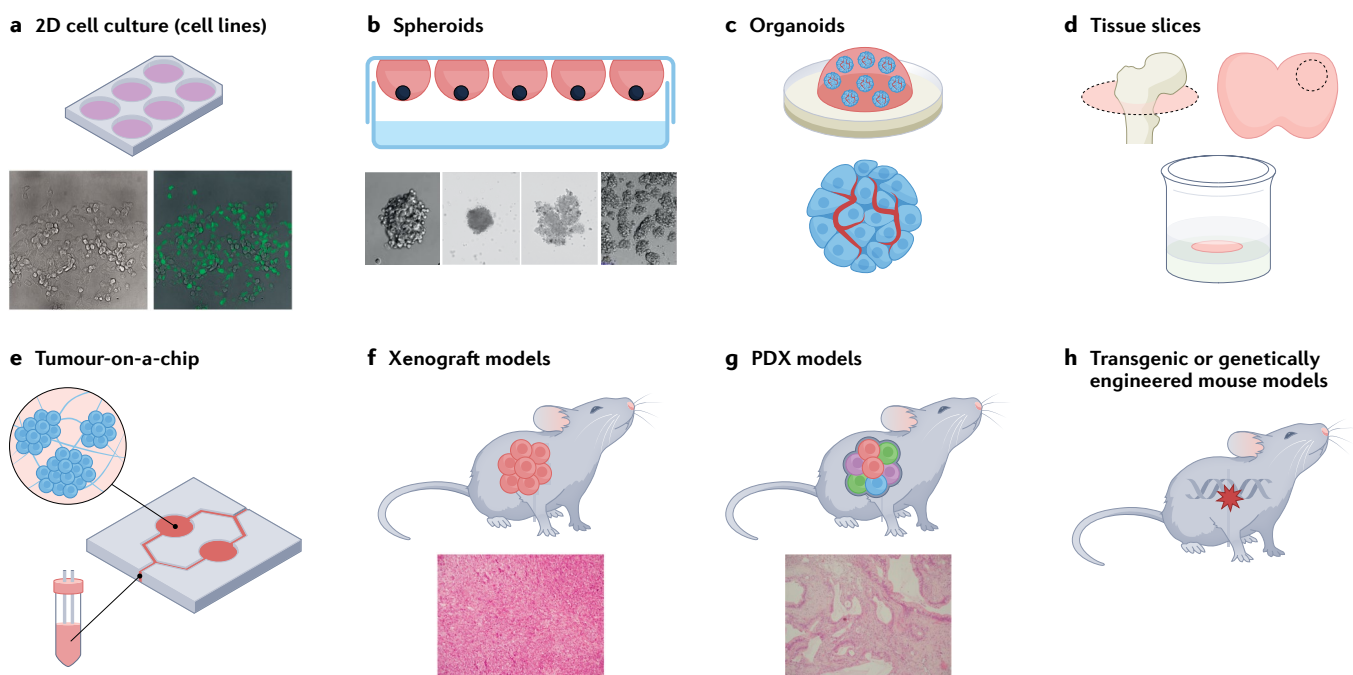


Fig. 2 | Overview of various models in prostate cancer research. Beyond classical 2D cell culture (part a), numerous 3D *in vitro* and *ex vivo* models exist. These models include different spheroid (part b) or organoid (part c) cultures as well as *ex vivo* tissue slice systems in an air–liquid interface (ALI) setting (part d). Tumour-on-a-chip (part e)

systems (part e) are aimed at mimicking the *in vivo* situation more closely. *In vivo* models mostly employ mice and can be based on xenografted tumour cells (part f), patient-derived xenografts (PDXs) from tumours (part g) or various transgenic or genetically engineered mouse models (part h).

pressure exerted by multiple therapy types in the setting of CRPC⁷⁰. Organoids might be of considerable value in the discovery of therapeutic targets and validating them in a high-throughput approach⁷³. However, the success rate of establishing continuously propagated organoid lines from metastatic prostate cancer was found to be only ~15–20%, although initial efficacies for 1–2-month short-term cultures were higher, depending on the site of the biopsy. Approximately 70% of tumour samples from soft tissue and ~30% of tumour samples from bone were successfully cultured for 1–2 months⁷⁰. This switch was hypothesized to occur because tumour cultures were overtaken by tumour-associated spindle cells or nonmalignant epithelial cells from the biopsy material, suggesting that strategies to selectively isolate tumour cells from the ‘contaminating’ nonmalignant epithelial and stromal cells could be beneficial. In addition, organoid cultures are expensive and labour intensive, and require an elaborately organized workflow to procure fresh tissue immediately after a biopsy or surgical procedure⁷³. Obtained organoid lines have been shown to recapitulate the molecular diversity of prostate cancer subtypes, with a mutational landscape similar to primary prostate cancer, including loss of *TP53* and *RB* tumour suppressor pathway function as the most common feature shared across the organoid lines⁷⁰. Clinically, the combination of these alterations leads to a particularly aggressive prostate cancer variant.

Scaffold-based systems

Spheroid and organoid models can also be extended towards scaffold-based systems. Extracellular matrix (ECM)-like gels – such as Matrigel, collagen and alginate – that are generally based on highly hydrophilic polymers, can be employed and can have stiffness that recapitulates soft tissue⁷⁴. Use of these gels usually leads to spontaneous aggregation of prostate cell cultures in the gel with both cell–cell and cell–matrix contacts. Matrigel is used most often and is considered the gold standard, despite issues of batch-to-batch variability and the inherently complex composition of this ECM-like gel. However, these issues can complicate assessment of cellular readouts with effects of matrix composition, and evidence suggests that Matrigel hampers drug response, resulting in potentially compromised organoid reaction to drug testing. For instance, cells in the core of the organoid show a different drug reaction from those at the periphery. Furthermore, AR translocation is altered, potentially resulting in false-negative read-outs⁷⁵.

Other synthetic or semi-synthetic matrices have been employed in addition to Matrigel. Synthetic materials are inert and, therefore, enable the controlled addition of defined ECM protein and tumour cells to deposit their own natural matrix. However, the presence of crucial matrix components must be ensured, including collagen, laminins, fibronectin and proteoglycans, which are biologically relevant.

Polyethylene glycol (PEG) modified with hyaluronic acid (HA-PEG) and then further grafted with the tripeptide RGD (Arg-Gly-Asp) has been successfully used for cultivation of PDX-derived prostate cancer cells⁷⁶. This approach is of particular interest as PDX-derived tumour cells, for example, the PDX-derived LuCaP series, often fail to adhere and to grow in standard 2D cell culture³². The encapsulation of the PDX tumour cells within a 3D hyaluronan-based hydrogel maintained PDX cell viability with continued native AR expression. Notably, these cells were largely resistant towards docetaxel, whereas the bone metastatic prostate cancer cell line C4-2B, encapsulated in an identical hydrogel, showed sensitivity⁷⁶, indicating that the source of the cells (PDX versus stable cell line) rather than the encapsulation process is the major source of differences in drug sensitivity and highlighting the translational importance of cell systems beyond established cell lines.

However, matrix effects on chemotherapy sensitivity have also been observed. A 3D glycosaminoglycan-based hydrogel culture system was used to monitor tumour vascularization by the formation of a bioengineered tumour angiogenesis microenvironment⁷⁷. In this study, a matrix metalloproteinase (MMP)-sensitive four-arm star-shaped PEG (starPEG)-heparin hydrogel system was established that incorporated RGD motifs at a defined density as binding sites for cells via integrins and MMP-responsive sequences to enable cells to locally remodel the matrix for the purposes of proliferation and migration. Notably, when this system was used to support different cell types including LNCaP or PC3 prostate cancer cell lines, HUVEC endothelial cells and mesenchymal stromal cells, the cells were found to be more resistant to chemotherapy than 2D cell cultures, more closely resembling, therefore, the *in vivo* situation in terms of tumour regression. Notably, this system can recreate prostate tumour vascularization and, therefore, even enabled study of the effects of angiogenesis inhibitors⁷⁷.

Prefabricated scaffolds, consisting of porous natural polymers (such as chitosan or collagen) or synthetic polymers (for example, polycaprolactone) can also be used to provide physical support for spheroids and the otherwise missing ECM.

Evidence of bone metastases is present in >90% of patients with advanced prostate cancer⁷⁸ and, therefore, 3D models have been established to mimic osseous metastasis. These so-called hard scaffolds, in particular, medical-grade polycaprolactone, are used for engineering bone tissue-like systems. As this polymer has a low melting point, it is printed in a microfibre 3D architecture whereby linear or tubular porous scaffolds are prepared from melt electrospinning combined with additive manufacturing (collectively termed ‘melt electrowriting’) and populated with primary osteoprogenitors isolated from human bone tissue⁷⁹. Further coating of the fibres with calcium phosphate and the use of osteogenic differentiation media resulted in microtissues containing osteoblasts and osteocytes. These scaffolds have been used as a mineralized model platform for studying prostate cancer growth in bone, by co-culturing cancer cell lines (LNCaP, C4-2B, PC3)⁸⁰ or PDXs⁷⁹. Treatment with the AR inhibitors enzalutamide or bicalutamide demonstrated that these microtissue-engineered models of mineralized metastatic tissue are useful for studying the bone TME and responses to therapies for mCRPC⁸¹. A 3D melt electrowritten medical-grade polycaprolactone scaffold system has also been used for cultivating primary patient-derived cancer-associated fibroblasts (CAFs). In this model, CAF deposition of extensive ECM promoted considerable changes in prostate epithelial morphology, in contrast to fibroblasts that were not associated with malignancy. This effect was further enhanced by the addition of mast cells via a tryptase-mediated mechanism. Thus, this system was useful for identification of defined interactions between prostatic CAFs, their native ECM and mast cell-derived tryptase as important microenvironmental drivers of prostate cancer progression⁸².

Tissue cultures and microfluidic platforms

Ex vivo tissue slice cultures enable the monitoring of the behaviour and therapeutic response of cancer cells during their cultivation after extraction from humans (patient derived) or xenografts (xenograft derived)^{83,84}. From humans, tumour material from both radical prostatectomy^{85,86} and transurethral resection of the prostate as well as prostate cancer bone metastases⁸⁷ have been successfully used for tissue slice models. However, implementation of tissue slice models is limited by the small sample sizes available for research after tissue processing for diagnostic purposes. In particular, this lack of tissue limits the use of metastatic and castration-resistant specimens.

Unlike primary cell cultures and 2D or 3D models, tissue slice culture systems preserve the morphology and microenvironment of the original tumour^{86,88}, and tumour heterogeneity and tumour–stromal interactions are also maintained as much as possible. In order to generate tissue slice cultures, the tumour is cut into thin slices immediately after surgery and cultured in fetal calf serum-containing medium on cell culture inserts. This strategy requires rapid processing of the tissue specimens after surgical removal. Using this approach, intact tumour tissue can be cultivated ex vivo as organotypic tissue slices in air–liquid interface culture for several days. Tissue slice cultures have been established from a variety of primary tumours including head and neck squamous cell carcinoma⁸⁹, human gastric and oesophagogastric junction cancer⁹⁰, colorectal carcinoma⁹¹ and others. Glioblastoma tissue slices, for example, were shown to be viable under these conditions for up to 14 days⁹². Generation of thin, precision-cut tissue slices and their implantation under the renal capsule of immunodeficient mice with subsequent ADT and analysis of the recovered tissue slices have also been reported to be successful⁸⁵. In order to perform drug screens, tissue slice models require rapid establishment after surgical removal of the tumour, and optimization of culture conditions in order to avoid cell damage and tissue necrosis⁸⁶. These conditions enable the measurement of drug response and cytotoxicity, in a setting that closely resembles the situation found *in vivo* (Box 1). After implementation of the culture system, tissue sections are treated with drugs or exposed to defined conditions, for example hypoxia, followed for example by paraffin-embedding and subsequent morphological and immunohistochemical evaluation and molecular analysis⁸³.

Tumour tissue slices have also been cultivated using microfluidic platforms, whereby fluid flows through micrometre-sized domains. In this study, an optimized cancer-on-chip platform was used to maintain viability and sustained proliferation of tissue slices derived from a prostate PDX for 7 days⁹³. Importantly, the system also accurately monitored

sensitivity towards the non-steroidal anti-androgen apalutamide⁹³. Microfluidic devices can use micro-dissected tissue – submillimetre-sized tissue sections from surgical or biopsy samples – to address the issue of limited patient tissue availability, which can be loaded, trapped and incubated within a microfluidic device⁹⁴. Microdissected tumour tissue has been shown to preserve tumour cell viability and proliferation better than tissue slice cultures, although slices demonstrated reduced hypoxia when cultured in microfluidic devices⁹⁵. In a study using tumour tissue from prostate cell line xenografts (PC3 and 22Rv1)⁹⁴, preservation of viability and integrity of micro-dissected tissues derived from tumour tissue from the xenografts was demonstrated over a period of at least 8 days and was also shown in one prostate cancer and one benign prostatic hyperplasia tissue sample⁹⁴.

Microfluidic devices in combination with micro-electro-mechanical systems can integrate several components of an intact tumour environment and have been employed for studying various tumour entities such as lung, brain, breast, urinary system, intestine, liver and others⁹⁶. They rely on perfusion, providing steady-state culture conditions with continuous nutrient supply and waste removal, realistic shear stress, and the possibility of precise time-dependent application of test drugs. Microfluidic devices have often been referred to as tumour-on-a-chip systems, but when co-culturing the tumour in parallel with other organ cultures, they can support more complex systems, which might be considered to represent ‘human-on-a chip’ or ‘body-on-a chip’ systems. These complex microfluidic systems can, for example, include study of pharmacokinetic properties, enabling accurate prediction of drug efficacies and adverse effects on other organs.

Microfluidic platforms have also been used to reduce the time periods needed for drug screening. In one study, a 3D microfluidic platform for potential use in real-time (<12 h) analysis of outcomes associated with chemotherapy was described, which was based on a platform in combination with microsensors for measuring changes

Box 1

Tumour slice models in drug research

Most studies in prostate cancer are aimed at investigating the response to different clinically approved standard therapies and serve as validation experiments for tumour slice models. Prostatic tissue slice models have been established and demonstrate properties characteristic of prostate cancer, such as sensitivity to androgen deprivation therapy and response to hypoxia or extracellular calcium⁸⁶. The response of tissue slices from patient-derived xenografts with different BRCA-status and androgen receptor (AR) levels to treatment with enzalutamide and the PARP inhibitor olaparib was shown to recapitulate *in vivo* findings⁸⁸. Tumour slices of xenografts from three patient-derived xenograft mouse models with different AR expression levels and different BRCA2 status were employed to optimize culture conditions, with tissue viability being maintained for at least 6 days. Enzalutamide treatment led to reduced proliferation, increased apoptosis and decreased AR expression and PSA secretion in AR-expressing tumour slices, but not in their AR-negative counterparts. Likewise, olaparib effects were confined to BRCA2-mutated tumour slices⁸⁸. Similarly, xenograft-derived tissue slices were shown to respond to docetaxel with

increased apoptosis, as determined by cleaved-caspase 3 levels⁸⁷. Evidence also shows successful gene induction and subsequent drug-response monitoring in a tissue slice model: tissue samples of human BPH were cultured *ex vivo* on gelatin sponges and transduced with lentiviral particles for inducing the expression of ING3 (ref. ²²⁸). Subsequent tissue analyses after paraffin embedding enabled exploration of the pleiotropic role of ING3 in carcinogenesis and its function as an oncogene. Tissue slice air–liquid interface cultures have also been used for studying nanoparticle effects: in tissue slices from PC-3-based xenograft tumour material, nanoparticles based on polyethylenimine for short interfering RNA delivery resulted in ~50% target gene (*BIRC5*) knockdown in the tumour tissue. As tissue slice cultures recapitulate the intact natural tumour architecture, the results of this study also indicated that nanoparticles can penetrate the prostate tumour tissue, even in the absence of microvessels and physical stimuli²²⁹. By analysing enhanced green fluorescent protein reporter gene expression upon nanoparticle-mediated DNA transfection, this effect was also seen on confocal microscopy of sections taken from tissue slices²³⁰.

in the electrical response of DU 145 cells seeded in a 3D ECM upon addition of a cytostatic drug. The impedance change was observed to differ between susceptible and resistant cells, enabling the distinction between drug-susceptible cells, drug-tolerant cells, and drug-resistant cells in a short time period⁹⁷.

Chorioallantoic membrane models

Finally, the CAMs of fertilized chicken eggs have been used as substrate for 3D tumour growth. As CAM assays are performed in the early phase of embryonic growth, they provide a test system that is not considered to be a full animal experiment. Inoculation of the CAM with prostate cancer cell suspensions led to the formation of 3D tumours, which were associated with profound neoangiogenesis. Intravenous injection of a test substance (the phorbol ester 12-O-tetradecanoylphorbol-13-acetate) also demonstrated the applicability of the CAM model as a test system for early *in vivo* cancer research⁹⁸.

Tumour xenograft models

Tumour xenograft animal models are aimed at bridging basic and clinical research and supplementing the use of *in vitro* model systems. They involve the implantation of prostate cancer cells or tissues into the body of an experimental animal, in most cases mice, and can be classified into subcutaneous, subrenal or orthotopic xenograft models.

Subcutaneous xenografts

Classical models for human prostate cancer consist of immunodeficient mice carrying subcutaneous prostate cancer cell line xenografts, generated by injection of cultured cells (for example, LNCaP, PC3 or DU 145 and their sublines)⁹⁹ or co-injection of cultured prostate cancer cells and stromal cells^{100–102}. For increased tumour take efficiency, cancer cells can also be injected using a carrier matrix such as Matrigel. After cell implantation, tumours can be palpated within an average of ~2–6 weeks, depending on the aggressiveness and/or tumorigenicity of the cell line and *in vivo* growth rate, which can be assessed by measuring the tumour dimensions from the outside. As cells are derived from cell culture, they can be pre-treated or genetically modified before injection, for example, by stable transfection to induce gene knockdown¹⁰³. Beyond addressing fundamental questions of prostate cancer biology, xenograft models have also been employed in drug studies^{104–106}. For example, this model has been used to show that the histone methyltransferase KMT9 controls growth of PC-3M, LNCaP and LAPC4-EnzaR xenografts, validating KMT9 as a novel target for the treatment of CRPC and enzalutamide-resistant prostate cancer¹⁰⁷.

Although such cell line xenograft models are valuable for basic studies, their ability to predict anticancer drug efficacy in the clinical milieu is limited¹⁰⁸. These limitations seem to be a result of high levels of homogeneity and the transcriptome alterations⁶³ of established cell lines after long-term *in vitro* culturing, compared with the heterogeneity and expression profiles of primary tumour specimens. Furthermore, cell line xenografts in mice do not possess the human tissue architecture of the original cancer specimens from which the cell lines were originally derived. Consequently, despite the presence of murine non-tumour components in the xenograft (including fibroblasts, endothelial cells and stroma), they do not accurately represent the complex interactions between the cancer cells and various components of their microenvironment, as found in the original malignancies. Even so, subcutaneous xenograft experiments do mimic several important features of *in vivo* tumour growth, such as proliferative response to androgens or androgen-independence, improving on data

obtained from *in vivo* cultures of prostate tumour cells. Xenografts are also easy to establish, with comparatively low costs, and changes in tumour size can be readily monitored.

Subrenal xenografts

Subrenal grafting is the process of recombining prostate cancer cells with rat urogenital sinus mesenchymal cells and then transplanting this recombinant tissue beneath the kidney capsule in immunodeficient mice¹⁰⁹. This method is used to assess the growth and investigate the ability of putative basal-like prostate stem cells from either the nonmalignant mouse prostate or mouse prostate cancer tissues to generate prostatic tissue.

Results have demonstrated efficient *in vivo* regeneration of prostatic structures in the subcapsular space of the kidney within 4–8 weeks. The regenerated structures showed a branching tubular epithelial morphology, with expression of a panel of markers such as AR, p63, PSCA and DLP-1 consistent with prostate development¹¹⁰. A procedure for successfully grafting and serially transplanting primary human prostate cancer tissues in SCID mice has been developed; using the subrenal capsule graft site and with adjustment of the hormonal status of the host mice, tumour take rates of >95% were achieved¹¹¹.

A conditional *Pten*-deletion mouse model has been used in renal graft experiments to show that prostate cancer stem cells mixed with CAFs produce prostatic glandular structures with numerous lesions, a high proliferative index and tumour-like histopathologies¹¹². This model has also been used to show that luminal cells expressing the homeobox gene *Nkx3.1* in the absence of testicular androgens are bi-potential, can self-renew *in vivo* and can reconstitute prostate ducts in renal grafts¹¹³. Implantation of xenografts under the subrenal capsule provides a better microenvironment than subcutaneous models and a higher engraftment rate than orthotopic xenografts, but this implantation method is technically challenging and demands elaborate tools to control *in vivo* growth.

Orthotopic xenografts

Orthotopic xenografting was introduced in an attempt to improve recapitulation of prostate at its actual pathophysiological site¹¹⁴. Orthotopic xenograft models provide a useful approach for understanding the specific interactions between genetically and molecularly altered tumour cells and their organ microenvironment, and for the evaluation of efficacies of therapeutic regimens^{115–119}. These models faithfully recapitulate the organ-specific microenvironment and facilitate analyses involving tumour–stromal interactions that are crucial for developing new-generation cancer therapies. The models enable monitoring of tumour progression and metastasis development. This method has been used to generate PC-3 and LNCaP lineages, which were discovered to metastasize to lymph nodes, lung and bone^{120–122}.

As human cell lines require immunodeficient mice as a host for xenografting, effects and contributions of immune cells cannot be monitored. However, in orthotopic xenograft models, the use of immunocompetent mice and murine cells can help to investigate the role of the immune system in tumour growth. For example, co-implantation of mouse prostate cancer MPC3-luc cells with T helper 17-polarized mouse splenocytes in the prostate of immunocompetent C57BL/6J male mice has been shown to promote orthotopic allograft prostate tumour growth¹²³. Novel orthotopic models, such as the transgenic adenocarcinoma of the mouse prostate (TRAMP)-derived orthotopic prostate syngenic mouse model, have been developed for monitoring tumour and metastatic responses to novel treatments¹²⁴. However,

unlike subcutaneous xenograft models, orthotopic mouse models require elaborate techniques and are relatively costly, and one of the crucial challenges in subrenal and orthotopic models is the real-time tracking of tumour growth. Ultrasonography and bioluminescent imaging of luciferase-expressing or green fluorescent protein-expressing cell lines have been successfully implemented to track murine tumour growth^{122,124,125}.

Patient-derived xenografts

The overarching principle of PDXs is the direct transplantation of freshly isolated tumour tissue, such as that from a primary or metastatic lesion, from a patient into immune-compromised mice, using subcutaneous implantation in the flank as the preferred strategy¹²⁶. This technique is also used to generate PDX models of neuroendocrine prostate cancer¹²⁷. In contrast to stable cell lines or genetically modified mice, PDX models should embody the unique mutational profile and heterogeneity of the original tumour and, therefore, have the potential to be used to personalize treatment to individual patients. At present, the generally low take rates and long latency periods in recipient animals impede routine clinical use of PDX models¹²⁸. However, several stable individual PDXs have been propagated in specific test animals, offering repetitive testing, and are available to the scientific community. Treatment responses of tumour-bearing mice commonly reflect the responses in cancer patients^{129–133}. Especially in the field of drug testing, these newly developed PDX models have paved the way for the discovery of previously unknown molecular principles and deregulated pathways^{134–136}. Additionally, establishment of cell lines from PDX tumours has been attempted; however, this approach has been associated with low success rates, as seen in the case of the LuCaP series, in which only one out of six xenografts has been successfully transformed into a stable cell line³².

From a technical point of view, handling PDX models is complex and variations in tumour engraftment, drug dosing, and response assessment protocols can affect the outcomes from different laboratories, making comparison difficult¹²⁸. Thus, experimental procedures that maintain robustness as well as standardized cloud-based workflows for PDX exome-sequencing, RNA-sequencing analyses and tumour growth evaluation are envisaged¹³². Whether engrafted PDXs undergo mouse-specific tumour evolution is the subject of an ongoing debate. Initially, reports suggested that PDX models were subject to a rapid accumulation of copy number alterations (CNAs) and that several CNAs that are often observed in primary (human) tumours gradually disappeared in PDXs. These results indicate that events undergoing positive selection in humans cannot necessarily be observed during propagation in mice¹³⁷. However, a subsequent study did not confirm CNA differences between patient and PDX tumours. By contrast, comparable variations in multi-region samples within patients were observed in this study, but this result does not rule out the possibility that PDXs can evolve in individual trajectories over time¹³⁸.

In principle, tumour development is controlled by an immune response involving cytotoxic innate and adaptive immune cells. Engraftment rates of PDX models increase after transplantation into immunocompromised mice¹²⁶, whereas recipient mice with an intact immune system would be required in order to analyse tumour-immune system interaction and the evaluation of immunotherapy response. Thus, the use of so-called humanized mice for xenograft transplants has the potential to further elucidate the mechanisms of immune response and might accelerate the discovery and development of immune-therapeutic agents¹³⁹.

In order to establish humanized mice, immune-deficient animals are engrafted with human stem cells that give rise to different lineages of immune cells in the test animals. The two mouse strains, NOD-SCID IL-2Rγ(null) mice and BALB/c-Rag1(null) IL-2Rγ(null) mice have been widely used to perform engraftment of human CD34-positive immune cells for this purpose¹⁴⁰. Humanized mice enable the investigation of the role of the human immune system in PDX growth, as well as the efficacy of immune-based therapies. However, only a few studies of translational prostate cancer research in these models have been published^{141,142}, which might be related to the high cost of these models. On the background of the TRAMP model, two examples of humanized mice have been established by expression of native human NKG2D ligand MHC class I polypeptide-related sequence B (MICB) or the engineered membrane-restricted MICB (MICB.A2)¹⁴³. Beyond PDXs, these models might have the potential to be used for studying and optimizing cancer immunotherapy, because these models develop spontaneous carcinomas. However, a drawback is that these models recapitulate only the specific interactions between NKG2D and its cognate ligands.

CTC eXplant models

Circulating tumour cells (CTCs) are another powerful tool for translational cancer research and personalized cancer therapy¹⁴⁴. In 2020, a CTC-derived eXplant (CDX) and a corresponding CDX-derived cell line were successfully established from a diagnostic leukapheresis (DLA) product. This CDX is a new model for studying the sequential acquisition of key drivers of neuroendocrine transdifferentiation and offers a unique tool for effective drug screening in neuroendocrine disease (castration-resistant neuroendocrine prostate cancer) management¹⁴⁵. However, although cell line models are important tools in basic cancer research, success rates in culturing CTCs are very low and, therefore, this approach cannot be used to determine personalized therapies for the management of individual patients. Increasing CTC capture rates¹⁴⁶ might help to increase the chance of being able to culture CTCs. Notably, the DLA method enables CTC capture from large blood volumes and has also been the basis for establishing organoids from enriched CTC fractions, indicating that DLA offers a promising alternative to biopsy procedures for obtaining sufficient numbers of tumour cells to study sequential samples in patients with metastatic prostate cancer¹⁴⁷. Thus, these cells can be also studied in 3D using in vitro systems like spheroid cultures^{148,149}, which are also used for other patient-derived cell culture models useful for translational research. Nevertheless, prostate cancer cells are notoriously more difficult to culture than cells from other tumour types.

Transgenic and genetically engineered mouse models

The Mouse Genome Database (MGI 6.17) currently lists 58 different genetically engineered mouse models (GEMMs) with phenotypic similarity to human prostate cancer. Several research groups have developed transgenic mouse models that recapitulate prostate cancer progression. These models use the expression of transgenic and oncogenic genes or gene fragments under the control of a prostate-specific promoter, mostly the probasin gene (*Pbsn*)^{150–152}. According to this principle, the TRAMP model exploits orthotopic expression of the SV40 large tumour T antigen. TRAMP mice are a versatile model for studying different disease stages, which are dependent on the age of mice. By 12 weeks of age, TRAMP mice exhibit prostatic intraepithelial neoplasia (PIN). By 18–20 weeks, tumour lesions are apparent

predominantly in the dorsal and lateral lobes of the prostate. After 28–32 weeks, all TRAMP mice usually develop advanced disease, encompassing lymph node and distant metastasis formation¹⁵³. A transgenic mouse model developed in 2020 uses prostate-specific overexpression of the transmembrane CUB domain-containing protein 1 (CDCP1). These mice develop a high penetrance of PIN between 7 and 9 months of age. In the initial study, this model was used to establish a molecular link between *CDCP1* over-expression with *PTEN* loss, for promoting prostate cancer progression through the upregulation of the MAPK pathway¹⁵⁴. Although no further studies using this model have been published, this model might be appropriate for studying the emergence of metastases and CRPC in a different context.

The MYC-driven murine prostate cancer model (Hi-Myc) is another GEMM offering the opportunity to study different disease stages. In Hi-Myc mice, PIN lesions develop with essentially 100% penetrance within 2–4 weeks and progress with reliable kinetics to invasive adenocarcinomas after 3–6 months of age¹⁵¹. Although distant metastasis is not observed in Hi-Myc mice, crossbreeding with mice harbouring haploid NF-κB inactivation generates offspring that can be used to study progression to castration-resistant disease¹⁵⁵. In addition, the JOCK1 GEMM uses a composite probasin promoter (ARR2PB) for orthotopic expression of *Fgfr1*. In this model, forced *Fgfr1* expression leads to the development of PIN, but not of cancer, within 30 weeks in test animals¹⁵². In order to drive this PIN into metastatic disease, a delayed treatment with a chemical inducer of dimerization (AP20187) is applied and, from 42 weeks onwards, mice develop penetrant adenocarcinomas. Interestingly, in this model, the stepwise and reversible progression to metastatic disease is linked to epithelial-to-mesenchymal transition (EMT), which can help to explain invasive and metastatic behaviour at different EMT stages, as in vivo EMT models for prostate cancer are scarce. However, the authors also point out that the promoter driving expression of the FGFR1 construct could be active at low levels in the stroma as well, possibly contributing to the observed changes by driving the development of the sarcomas observed in the model.

Complete inactivation of *Nkx3.1*, the expression of which is mostly restricted to the prostate, provides an animal model for examining the relationship between nonmalignant prostate differentiation and early stages of prostate carcinogenesis. At 1 year of age, homozygous male mice show extensive hyperplastic epithelium at the anterior of the prostate¹⁵⁶. When *Nkx3.1*-null mice are crossbred with mice harbouring *Pten* inactivation, the animals develop high-grade PIN and early adenocarcinomas by the age of 6 months¹⁵⁷.

A transgenic mouse line that expresses the cre recombinase gene under the control of the composite probasin promoter provides the basis for many other GEMM with prostate-epithelial-cell-specific gene ablations. A *Pten*-conditional knockout model recapitulates disease progression seen in humans, starting with PIN, followed by progression to invasive adenocarcinoma and subsequent metastasis. These mice are a versatile model for studying the molecular mechanism and therapeutic strategies of prostate cancer¹⁵⁸.

Mouse models combining *Pten* inactivation with other drivers of prostate cancer progression enable investigations with increased focus. Thus, combining a conditional deletion of *Ar* is useful for analysing crosstalk between the PI3K and AR pathways and CRPC development¹⁵⁹. In this setting, the combination of a conditional *Pten* heterozygous background with prostate-specific conditional expression of *Spop*^{F133V} – a common missense mutation found in human prostate cancer – led to profound alterations in phenotypes and provided models for analysing both PI3K-mTOR and AR pathways¹⁶⁰. In another model, a combination

with *Trp53* deletion and telomere dysfunction yields a GEMM of aggressive cancers with rearranged genomes and bone metastasis formation¹⁶¹. Crossing conditional activatable KRas (G12D/WT) mice with the prostate conditional *Pten*-deletion mice generates a model of macrometastatic prostate cancer with EMT, stem-like features and 100% penetrance¹⁶². In addition, prostate-specific overexpression of *Cdcp1* in transgenic mice cooperates with the loss of *Pten* to promote the emergence of metastatic hormone-sensitive and hormone-resistant disease¹⁵⁴. Furthermore, over-expression of *Mycn* in *Pten*-null mice established a mouse model that develops poorly differentiated, invasive prostate cancer that is molecularly similar to human neuroendocrine prostate cancer¹⁶³ and another group has created several different mouse models that enable testing of immune therapies in prostate cancer. Deletion of *Smad4* in a *Pten*-null background already provides a mouse model of metastatic prostate cancer with 100% penetrance¹⁶⁴, but additional deletion of *Chd1* is associated with remodelling of the TME accompanied by reduced numbers of myeloid-derived suppressor cells and increased CD8⁺ T cells¹⁶⁵. This mouse strain has successfully been applied for testing inhibition of interleukin 6 in combination with immune checkpoint blockade¹⁶⁵. The same group created a chimaera-based system, which is derived from mouse embryonic stem cells. Mice with prostate-specific homozygous deletion of *Pten*, *Trp53* and *Smad4* were crossed with reporter mice harbouring fluorescent protein and luciferase expression to create so-called CPPSML genotypes, which can be used to produce age-dependent fluorescent protein and chemiluminescent prostate cancer growth at 3 months of age. Use of this model to test immune checkpoint blockade combined with agents that neutralize myeloid-derived suppressor cells in primary CRPC and mCRPC showed positive responses to therapy¹⁶⁶.

Overall, transgenic or genetically engineered mouse models can be used to recapitulate different disease stages of prostate cancer (Table 2). The advantage of using these models, rather than xenografts, is the concomitance of an intact microenvironment and immune system, which serves the pressing need for models that enable testing of immune therapeutic agents. By contrast, interspecies conservation and, therefore, validation of findings in humans, is not always given. The development of mouse models that enable studies of bone metastasis formation remains a goal of the field²³.

Sophisticated models meet sophisticated analytics

All of the discussed model systems possess an intrinsic amount of complexity, which increases from 2D cell cultures and 3D organoids (tumour cells in contact with host cells) up to model systems with a fully retained morphology, such as tissue slice cultures, PDXs or genetic mouse models. Using systems with increased complexity enables analysis of the interactions of tumour cells with tumour stroma, and microenvironment including the host immune system. However, these advanced models also require advanced analytics.

2D cultures in combination with single-cell transcriptomics have been used to generate characteristic patterns of treatment-resistant subclones¹⁶⁷. Nevertheless, although single-cell approaches are immensely informative, they cannot display the spatial location of the cells they characterize. Methods exist that can incorporate information about the spatial distribution of the examined samples, for example, in one study the intratumoural and intertumoural heterogeneity of metastatic prostate cancer was analysed using digital spatial transcriptomics¹⁶⁸. However, spatial transcriptomics is limited to recapitulating morphology, and, therefore, simply provides another

Review article

Table 2 | Prostate cancer mouse models

Transgenic prostate cancer mouse models					
Transgene or mouse gene	Promoter or human gene	Allelic composition	Background strains	Key references	Characteristics and latency ^a
SV40 large T antigen	Pbsn	Tg(TRAMP)8247Ng	C57BL/6	150,153	PIN (-12 weeks) Adenocarcinoma (~19 weeks) Metastatic tumour (LN, visceral; ~30 weeks)
MYC	ARR2/Pbsn	Tg(ARR2/Pbsn-MYC)7Key	FVB/N	151	PIN (2–4 weeks) Adenocarcinoma (3–6 months)
FGFR1	Pbsn	Tg(Pbsn-Fgr1/Fkbp1a)#aDmusp/O treatment with AP20187	FVB/N	152,222	PIN (~30 weeks) Metastatic tumours (LN and liver; 42–52 weeks)
CDCP1	Pbsn	CDCP1 ^{pcLSL/+}	C57BL/6 × 129/Sv	154	PIN (7–9 months)
Genetically engineered prostate cancer mouse models					
<i>Nkx3-1</i>	NKX3-1	<i>Nkx3-1</i> ^{tm1Mms} / <i>Nkx3-1</i> ^{tm1Mms}	129S1/Sv 129S1/SvJmJ C57BL/6 J or 129S4/ SvJae C57BL/6	223	PIN (~12 months)
<i>Nkx3-1</i> <i>Pten</i>	NKX3-1 PTEN	<i>Nkx3-1</i> ^{tm1Mms} / <i>Nkx3-1</i> ⁺ <i>Pten</i> ^{tm1Rps} / <i>Pten</i> ⁺	129S1/Sv 129S1/SvJmJ C57BL/6 J	157	PIN (~6 months) Adenocarcinoma (~6 months)
<i>Pten</i>	PTEN	<i>Pten</i> ^{tm1Hwu} / <i>Pten</i> ^{tm1Hwu} Tg(Pbsn-cre)4Prb/O	129S4/SvJae BALB/c C57BL/6 DBA/2	158	PIN (9 weeks) Adenocarcinoma (12–29 weeks) Metastatic tumours (lung; 9–29 weeks)
Ar <i>Pten</i>	AR PTEN	Ar ^{tm1Verh} /Y <i>Pten</i> ^{tm1Hwu} / <i>Pten</i> ^{tm1Hwu} Tg(Pbsn-cre)4Prb/O	129S1/Sv 129S4/ SvJae 129 × 1/SvJ C57BL/6 DBA/2	159	PIN Adenocarcinoma Metastatic tumours CRPC
<i>Pten</i> <i>Tert</i> <i>Trp53</i>	PTEN TERT TP53	<i>Pten</i> ^{tm1Rdp} / <i>Pten</i> ^{tm1Rdp} <i>Tert</i> ^{tm3Rdp} / <i>Tert</i> ^{tm3Rdp} <i>Trp53</i> ^{tm1Bn} / <i>Trp53</i> ^{tm1Bn} Tg(Pbsn-cre)4Prb/O	129P2/OlaHsd 129S6/ SvEvTac C57BL/6 DBA/2	161	PIN (9 weeks) Adenocarcinoma (24 weeks) Bone metastasis (24 weeks)
Kras <i>Pten</i>	KRAS PTEN	Kras ^{tm4Tyi} / <i>Kras</i> ⁺ <i>Pten</i> ^{tm1Hwu} / <i>Pten</i> ^{tm1Hwu} Tg(Pbsn-cre)4Prb/O	129S4/SvJae C57BL/6 DBA/2	162	PIN (10 weeks) Adenocarcinoma (20 weeks) Metastatic tumours (lung, liver; 20 weeks)
<i>Pten</i>	PTEN	Gt(ROSA)26Sor ^{tm1(SPOP*)F133V} Mrbn/ Gt(ROSA)26Sor ⁺ <i>Pten</i> ^{tm2.1Ppp} / <i>Pten</i> ⁺ Tg(Pbsn-cre)4Prb/O	129S1/Sv C57BL/6 DBA/2	160	NA
<i>Pten</i> <i>Smad4</i>	PTEN SMAD4	<i>Pten</i> ^{-/-} <i>Smad4</i> ^{-/-} Tg(Pbsn-cre)4Prb/O	FVB/n C57BL/6 129/ Sv	164	Focal carcinoma (11 weeks) Invasive carcinoma (15 weeks)
<i>Pten</i> <i>Mycn</i>	PTEN MYCN	<i>Pten</i> ^{ff} LSL-MYCN ^{+/+} T2-Cre ^{+/+}	C57BL/6/129 × 1/SvJ	163	Invasive adenocarcinoma with NEPC

CRPC, castration-resistant prostate cancer; LN, lymph node; NEPC, neuroendocrine prostate cancer; PIN, prostatic intraepithelial neoplasia; SV40, Simian virus 40; NA, not applicable. ^aLatency indicates time until occurrence of the lesion (age of mice).

descriptive method without integration of functional analyses. To overcome this limitation, novel spatial transcriptomics have been developed. Some methods combine the advantage of high-resolution histological imaging with a full area-wise transcriptional analysis of the cells located directly above the capture area (the resolution depends on the size of the capture area)¹⁶⁹. This method has been used to correlate specific histomorphological features of primary prostate cancer with

transcriptional profiles of the tumour cells¹⁷⁰. Conversely, this method can also be used to identify the spatial localization of cells exhibiting a specific transcriptional pattern that has been previously identified¹⁶⁷. Sophisticated analysis methods will help not only to identify characteristic properties of tumour cells but also to characterize the interaction of tumour and microenvironment or monitor drug effects in an in vivo-like setting.

Review article

Table 3 | Comparison of various *in vitro*, *ex vivo* and *in vivo* models

Model	Description	Advantages	Disadvantages
2D <i>in vitro</i> cell culture (cell lines)	Submerged culture of cells, usually attached to a plastic surface	Easy handling, high reproducibility, enables different scales of culture, enables high-throughput screening, low costs	Artificial 2D surface, abnormal cell characteristics on the molecular and cellular level, does not monitor 3D growth conditions (cell–cell interactions, cell–stroma interactions)
Monocellular tumour spheroids	Cell line grown in culture that does not allow cells to attach to a surface, therefore leading to formation of cell clumps (spheroids)	Relatively easy handling, monitors cell–cell interactions between tumour cells and their 3D growth	Does not monitor cell–cell interactions between tumour and non-tumour cells, little control of cell aggregation, assessment of cell viability, less straightforward than 2D culture, no vasculature
Multicellular tumour spheroids	A mixture of tumour and non-tumour cells grown in culture that does not allow cells to attach to a surface, therefore leading to formation of cell clumps (spheroids)	Monitors cell–cell interactions between tumour cells and non-tumour cells, more realistic model of 3D growth than 2D models	Difficult to establish, difficult to distinguish drug effects on different cell types, little control of cell aggregation and spheroid architecture, no vasculature
Tumour-derived spheroids	Tumour-derived cells grown in culture that does not allow cells to attach to a surface, therefore leading to formation of cell clumps (spheroids)	3D system from primary tumour (tumour and non-tumour cells), patient specific	Restricted by tumour tissue availability
Tumour-derived organoids	Tumour-derived fresh tissue	In vivo-like architecture, patient specific, individualized high-throughput drug screening feasible	Elaborate workflow necessary, cost and labour intensive, low take rates of prostate cancer organoids
Organotypic tissue slices	Slices of tumour tissue (thickness in the hundred-micrometre range), cultivated, for example, in air–liquid interface	In vivo-like tumour architecture and microenvironment, patient specific	Limited cultivation time, monitoring of drug effects often requires microscopic analysis of tissue sections, restricted by tumour tissue availability
CAM models	Tumour cells or tissue grown on a chorioallantoic membrane of an egg	Reproducibility, particularly suited for monitoring angiogenesis, enables study of tumour growth and micrometastases	Short time window for experiments (implantation → chick hatching)
Tumour-on-a-chip systems	Combination of microfluidic technology and 3D cell culture	Faithful recapitulation of tumour microenvironment and interaction with cancer cells	Sophisticated tissue engineering, might not be suitable on a large scale
Tumour xenografts	Tumour cells subcutaneously, subrenally or orthotopically injected into a host animal (usually mice)	Monitors intact <i>in vivo</i> tumour environment, in particular subcutaneous xenografts comparably easy to establish with relatively low costs, also enables stromal cell co-injection	Animal experiment (3R), based on cell lines and murine cells, lacks immune system (immunodeficient mice) in the case of human cell lines, limited to tumorigenic cell lines
Patient-derived xenografts	Primary tumour material from a patient, implanted subcutaneously or orthotopically into a host animal (usually mice)	Original patient tumour material in an intact <i>in vivo</i> environment, many features of primary tumour material retained	Animal experiment (3R), low tumour take rates, long time period for establishment, slow tumour growth, restricted by tumour tissue availability, complicated handling
CTC eXplant model	Cells grow continuously in immune-compromised mice and as a stable cell line	Unique model that mirrors <i>in situ</i> CTC biology and overcomes the limitations of low frequency and durability of CTCs	Low success rates for establishment of models. Currently, only one model is available that is based on elaborate diagnostic leukapheresis
Transgenic or genetically engineered mouse models	Mice strains based on defined genetic modifications	Modelling individual steps of prostate tumorigenesis and metastatic progression. Enables study of the influence of microenvironment and immune system in longitudinal studies	Animal experiment (3R). Breeding mice is costly and labour intensive. Transgenic models can lack tissue specificity. Mice are not human and orthologous conservation is not always a given

3R, replace, reduce, refine (as a road map for laboratory animal protection policies); CAM, chorioallantoic membrane; CTC, circulating tumour cell.

Translating success from models to clinics

Many *in vitro*, *ex vivo* and *in vivo* models of prostate cancer are available, each of which is associated with defined advantages and disadvantages (Table 3). Prostate cancer progression and the development of therapy resistance are multistage processes that are shaped by numerous intrinsic and extrinsic factors; these factors create an ecosystem in which selection processes occur, but preclinical models are static and typically reflect a specific state of disease and not all common

features of prostate cancer are preserved (for example, PSA expression and AR expression).

2D cell culture is still the workhorse of prostate cancer research and drug development, but the field is moving towards more sophisticated models that more faithfully recapitulate key properties of the disease. These new models often involve the use of primary patient material rather than merely focusing on established cell lines. Indeed, in metastatic disease, a striking concordance of genomic alterations

in spatially distributed tumour sites is found⁹, especially in treatment-naïve, hormone-naïve prostate cancer¹⁷¹. Thus, a single biopsy from one metastatic site might be used to obtain information about the molecular make-up of the tumour and unravel targetable alterations. This finding provides the rationale for individualized cancer models derived from an individual's tumour tissue, such as PDOs, which have several advantages over 2D culture or 3D spheroids (Table 3). However, early branching evolution during metastatic dissemination and extensive subclonal heterogeneity in pan-cancer analyses have been found, especially when applying deep-sequencing approaches of multiple metastatic sites^{172,173}. In addition, under the sustained treatment pressure in the course of therapy, the formation of various resistance mechanisms, the development of new genetic drivers and subclonal

selection occur¹⁷¹. In these circumstances, a single biopsy can reflect only a limited extent of the actual disease and multiple biopsies would be necessary to capture the different facets of disease¹⁴⁴. In this scenario, cell models generated from CTCs could be a less invasive method than biopsy for the patient; however, challenges remain in realizing these models into use.

Overcoming challenges

Challenges in establishing patient-derived systems for personalized medicine arise from the need to procure fresh tissue, for example, from metastatic biopsy. Thus, a workflow to procure and process fresh tissue and a good communication protocol between surgeon and/or interventional radiologist, pathology and the cell culture laboratory must be in place. These procedures are personnel intensive and costly, and might not be feasible in all institutions and for all patients. In addition, success rates for establishing prostate cancer models based on primary tumour material are low in comparison with other tumour entities – for example, only ~20% of submitted prostate cancer tissue samples succeeded in forming organoids, whereas numbers are as high as 90% in other tumours, such as colorectal cancer^{73,174}. Enthusiasm for prostate cancer organoids remains, but the initial promise of bona fide ‘avatars’ modelling individual patients’ tumours for predictive drug testing has not been fulfilled. Instead, creating a ‘living biobank’ should be the goal to personalize prostate cancer treatment to enable predictive high-throughput drug testing. Furthermore, an organoid that is almost identical to the patient’s tumour on a genomic level could be selected for PDX development, combining precise genomic make-up with a living TME. This combined approach might offer an increasingly complex biological setting for drug sensitivity testing¹⁷⁵. Even so, drug testing is limited by other issues, including the definition of optimal readouts to drug response and the avoidance of false-positive or false-negative results.

The low success rate of prostate cancer samples in primary cell culture or PDX generation suggests a very strong dependence on signalling cues from the microenvironment¹⁷⁶, a concept that also applies to castration resistance. For example, using cells from a PDX model that can progress to androgen independence, bicalutamide and enzalutamide resistance were found to be considerably delayed and avoided altogether, respectively, when murine fibroblasts were removed from the cancer cell population. Interestingly, this effect was mediated by fibroblast-derived neuregulin 1, which activates the receptor tyrosine kinase HER3 in prostate cancer cells to promote survival signalling and to partially restore AR target gene expression, therefore conferring antiandrogen resistance¹⁷⁷. Although this finding further emphasizes the biological complexity of castration resistance, it also highlights the use of prostate cancer models to improve understanding of crucial disease processes.

The putative role of the microbiome

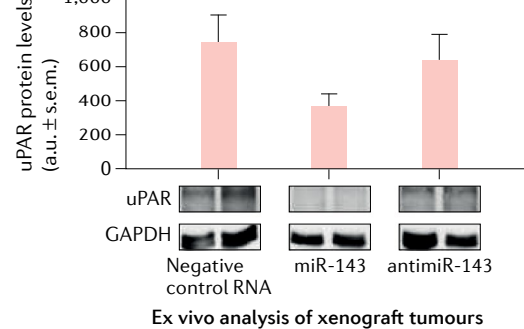
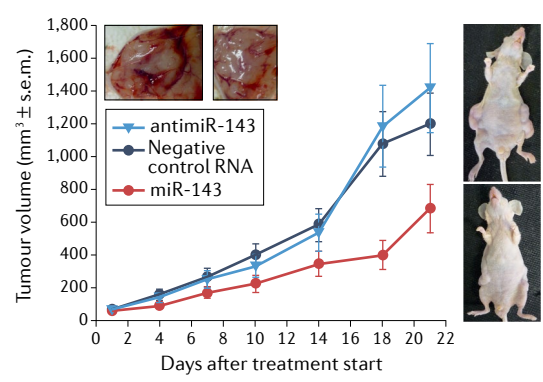
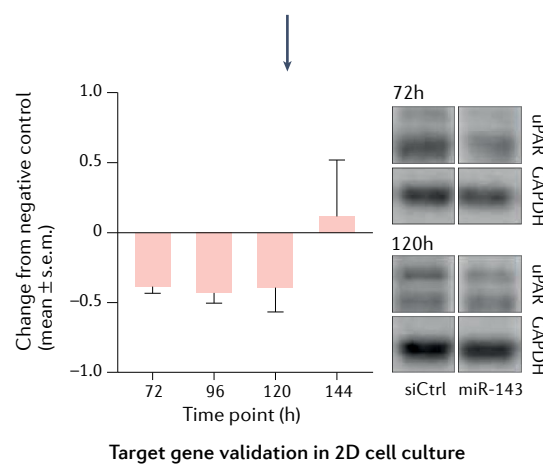
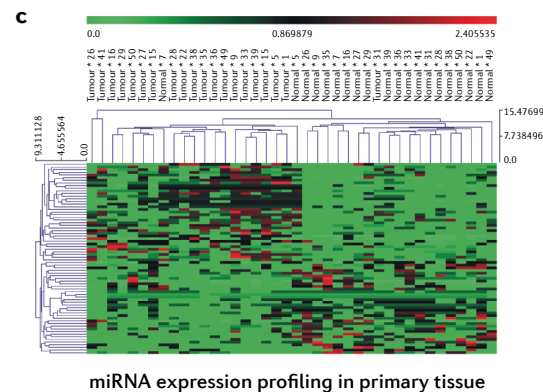
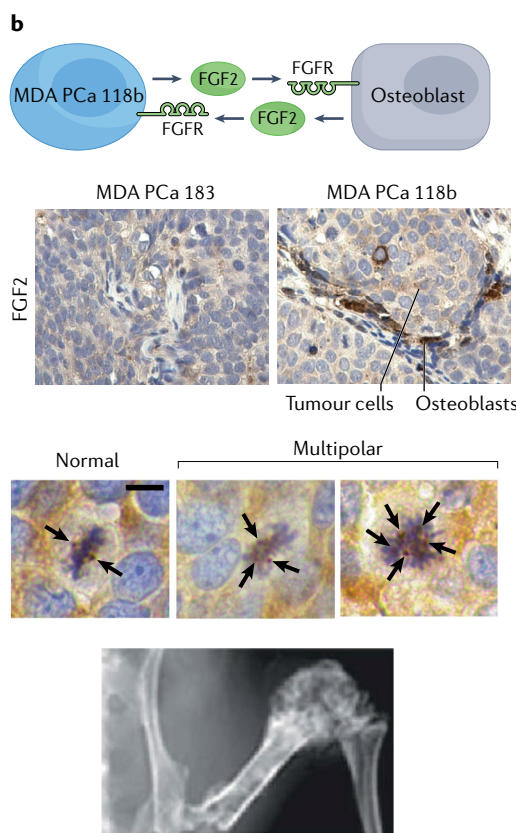
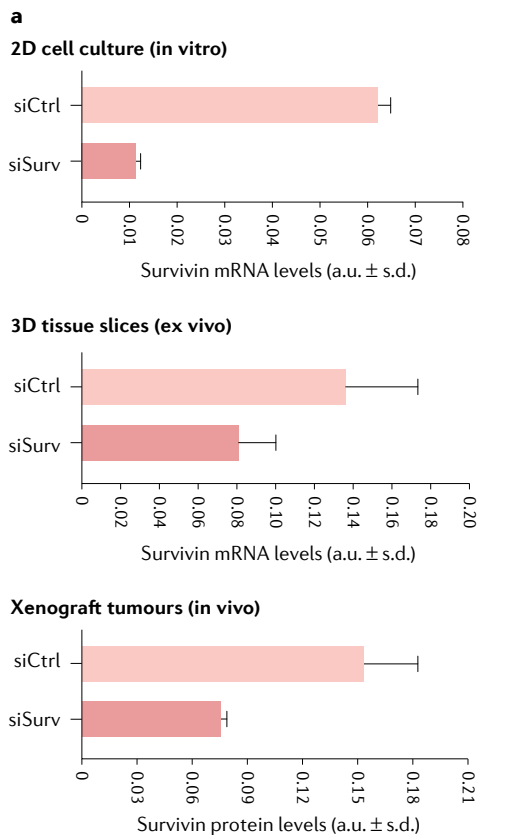
Interactions between prostate cancer and the prostate and gut microbiomes have been reported, increasing the complexity of prostate cancer¹⁷⁸. The presence of a prostate cancer microbiome is supported by data from The Cancer Genome Atlas showing that ~1.5% of sequence reads were of microbial origin¹⁷⁹. Treatment with the next-generation antiandrogen abiraterone has been shown to modulate the gut microbiome to enhance treatment effects¹⁸⁰. Conversely, gut microbiota have also been reported to promote castration resistance by converting hormone precursors to active androgens¹⁸¹. To study the influence of antihormonal agents on the gut microbiota, both *ex vivo* models such as bioreactors¹⁸⁰ and athymic or immunocompetent mouse models have been used. In the latter, co-housing of prostate cancer-bearing

Box 2

Androgen receptor splice variant 7

The successful interplay between *in vivo* and *in vitro* models can be observed in the case of the androgen receptor splice variant 7 (AR-V7) and its association with therapy resistance after treatment with abiraterone or enzalutamide. In the discovery of AR-V7, the mouse xenograft-derived cell line 22Rv1 (ref. ²³¹) (which was used for propagating the grafted prostate cancer primary tumour (CWR22) and for obtaining serial transplantable tumours) was used. Mice were kept under androgen ablation, resulting in establishment of the (CWR)22Rv1 hormone-refractory cell line²⁰⁷. Subsequent clinical studies in patients with metastatic castration-resistant prostate cancer showed AR-V7 to be a biomarker, predicting resistance to AR-targeted therapies abiraterone and enzalutamide, while not affecting the efficacy of a taxane-based chemotherapy^{232,233}. Detection of AR-V7 at the RNA or protein level was independently associated with short progression-free survival and overall survival of patients with metastatic castration-resistant prostate cancer treated with abiraterone or enzalutamide²³⁴. However, some patients responded to abiraterone or enzalutamide therapy despite the presence of AR-V7 mRNA-positive circulating tumour cells^{235,236}, indicating the need for AR-V7 re-assessment (for example, AR-V7 in plasma-derived exosomal RNA^{237,238}) or for additional predictive biomarkers (such as other AR variants) for safe clinical decision-making. Nevertheless, the presence of AR-V7-positive circulating tumour cells was associated with a short time to treatment change and might, therefore, provide important prognostic information²³⁹. AR-V7 positivity is associated with an increased proportion of Gleason score ≥8, metastases, and incidences of pain and worse Eastern Cooperative Oncology Group performance status (≥1) compared with patients with AR-V7-negative castration-resistant prostate cancer²⁴⁰. AR-V7 analysis has not yet reached routine clinical use, but this situation might change when selected clinical trials investigating AR-V7-targeting therapies provide positive results²⁴¹. However, emphasis must be put on the fact that castration resistance is a multifactorial process and tumour cells might rely on distinct molecular alterations to escape androgen deprivation, leading to clonal competition for dominance.

Review article



Review article

Fig. 3 | Examples of prostate cancer research, based on the combined use of different models. **a**, Comparison of nanoparticle and short interfering RNA-mediated knockdown of the proto-oncogene survivin in 2D cell culture, 3D tissue slices and xenograft tumours. Very profound target gene reduction is seen in 2D cell culture, but the 3D ex vivo model reflects the knockdown efficacies that are obtained *in vivo* more accurately (Karimov and Aigner, previously unpublished data). **b**, Schematic representation of a bone-forming prostate cancer patient-derived xenograft (PDX) model, in which human tumour cells (MDA PCa 118b) stimulate mouse osteoblasts through the FGF2–FGFR1 axis and vice versa (upper panel)²²⁴. Note that FGF2 is overexpressed in both cell types in comparison with a control PDX (MDA PCa 183, upper middle panels). The osteoblastic PDX model is characterized by a high mitotic index (not shown) and a high frequency of abnormal mitoses, as determined by spindle poles visualized by immunohistochemistry for γ-tubulin (lower middle panels). A radiograph

of the bone-forming PDX model is shown (lower panel). **c**, The typical workflow for identifying and validating microRNAs (miRNAs) as drug candidates. miRNA expression profiling in primary tumour versus nonmalignant tissue identifies aberrantly downregulated miRNAs (in this case miR-143). The *in silico* predicted or previously described target genes of potential relevance (in this case uPAR) are validated in 2D cell culture. A miRNA replacement study in subcutaneous tumour xenograft-bearing mice, using polymeric nanoparticles for miRNA formulation and delivery, reveals profound tumour inhibition. Upon their explantation, the tumours are analysed for expression profiles of miRNA target genes, here revealing the downregulation of uPAR in the specific treatment group. Part **b** from ref.²²⁴, reprinted with permission from AAAS, and adapted with permission from ref.²²⁵, Elsevier. Part **c** reprinted with permission from ref.²²⁶, Wiley, and adapted with permission from ref.²²⁷, American Society of Gene and Cell Therapy.

and non-tumour-bearing mice resulted in a substantial reduction of prostate tumour growth, improved responses to androgen deprivation, correction of immune cell dysfunction and a microbial shift towards microbiota that promote anticancer immune surveillance¹⁸². These remarkable findings have been attributed to the fact that mice are coprophagic; thus, faeces of non-tumour-bearing mice seem to be able to correct the cancer-induced gut dysbiosis and its consequences in tumour-bearing mice. These results emphasize the complexity of tumour–microbiome interactions and highlight the daunting challenge of faithfully modelling the ecosystem of prostate cancer.

Characteristics of tissue-slice and PDX models

Tissue-slice models offer experimental conditions that can recapitulate the TME and tissue compositions with increased accuracy. As the complexity of drug response is not only determined by intracellular parameters but also by features related to the microenvironment, tissue slices could emerge as promising models for drug development and for the identification of predictive biomarkers. However, their routine establishment is not without challenges, including limitations of tumour tissue availability, the preclusion of long-time experiments and the relative complexity of the method. So far, no standardized protocols exist, but such protocols are required for drug screens in the setting of personalized patient care¹⁸³. In principle, the issue of limited tissue availability can be circumvented by using PDX tumour material – that is, prior propagation of the patient’s tumour in mice. However, this step once again adds considerable complexity to the experimental setting, which is the case for all *in vivo* studies.

Intratumoural heterogeneity might also be a major confounding factor for PDX models. Synthetic DNA barcode tracking and single-cell transcriptomics have revealed spatially confined clonal expansion driven by cell-intrinsic overexpression of genes involved in homing and adhesion to the pre-metastatic niche¹⁸⁴. Such pre-existing differences in gene expression might influence not only the adaptation to the host microenvironment but also engraftment efficiency in general. Consequently, engrafted cells might not be representative of an entire tumour. Still, despite all 3R considerations, *in vivo* models will remain pivotal in prostate cancer research and drug development. One challenge will be to develop improved models for clinically relevant disease manifestations, such as *BRCA* positivity and therapy-induced neuroendocrine differentiation. Another unresolved problem is that of suitable models for the interaction between the immune system and prostate cancer – although immunotherapy has become integral to therapy of other cancer types, results in prostate cancer have been disappointing, mainly owing to its immunologically ‘cold’ tumour micromilieu. Attempts are now being made to activate inflammasome and immune cells by different methods such as various vaccination strategies¹⁸⁵. Resulting preclinical models could be more appropriate and could accelerate therapy development.

Artificial intelligence and preclinical models of prostate cancer

The major goals of preclinical prostate cancer models are not only to improve understanding of disease processes but also to identify novel treatment modalities and to predict treatment-related toxicities and therapy responses. Owing to the high degree of intertumoural and intratumoural heterogeneity, artificial intelligence (AI) has the potential to revolutionize multiple aspects of preclinical prostate cancer modelling.

Thus far, the use of AI in prostate cancer focuses mostly on decision-support, for example, deep-learning and pattern-recognition algorithms for MRI segmentation, histopathological grading or augmented reality in the operating room¹⁸⁶. Conceptually, AI can rely on big data for modelling individual patients ('digital twin'), or narrow-task approaches such as predicting the response to a certain drug¹⁸⁷. In the context of preclinical model development, one could envision that the role of artificial intelligence would be to strengthen the connection of *in vitro* or *in vivo* models and patient data. For example, the response to a drug candidate in a PDX model could be linked to the clinical patient information, imaging, digital pathology, tumour genomics and information on the clonal composition as well as heterogeneity of the tumour, gene expression data, and factors of the TME, including the immune response. The response or resistance to the compound could hence be integrated with data that might help to improve understanding and predict drug sensitivities as a basis for ultimately identifying patients who are likely to benefit from the drug. Moreover, AI can support virtually all aspects of preclinical drug discovery in model systems, including target identification, virtual drug screening and the prediction of pharmacokinetics and toxicity¹⁸⁸.

Conclusions

Despite substantial progress, the complexity of prostate cancer cannot yet be fully represented in a single preclinical model. A combination of different *in vitro*, *ex vivo* and *in vivo* models still provides the best approximation of the behaviour of prostate tumours (Box 2 and Fig. 3). Thus, new approaches and increasingly sophisticated models are needed to improve simulation of the individual phases of the disease and their underlying molecular and cellular drivers, in order to meet the requirements of therapy development and personalized medicine. This need is especially relevant in the case of immunotherapeutics, checkpoint inhibitors or CAR cell therapies, for which preclinical testing is particularly demanding. Successful strategies will also need to include AI and machine learning to identify specific molecular patterns of the disease, which might predict therapy response or resistance and will, therefore, require interdisciplinary approaches.

Published online: 30 November 2022

Review article

References

1. Siegel, R. L., Miller, K. D. & Jemal, A. Cancer statistics, 2020. *CA Cancer J. Clin.* **70**, 7–30 (2020).
2. Rebello, R. J. et al. Prostate cancer. *Nat. Rev. Dis. Primers* **7**, 9 (2021).
3. Siegel, R. L., Miller, K. D. & Jemal, A. Cancer statistics, 2018. *CA Cancer J. Clin.* **68**, 7–30 (2018).
4. Yamada, Y. & Beltran, H. The treatment landscape of metastatic prostate cancer. *Cancer Lett.* **519**, 20–29 (2021).
5. Antonarakis, E. S., Gomella, L. G. & Petrylak, D. P. When and how to use PARP inhibitors in prostate cancer: a systematic review of the literature with an update on on-going trials. *Eur. Urol. Oncol.* **3**, 594–611 (2020).
6. Sartor, O. et al. Lutetium-177-PSMA-617 for metastatic castration-resistant prostate cancer. *N. Engl. J. Med.* **385**, 1091–1103 (2021).
7. Litwin, M. S. & Tan, H. J. The diagnosis and treatment of prostate cancer: a review. *JAMA* **317**, 2532–2542 (2017).
8. Ali, A. et al. Prostate zones and cancer: lost in transition? *Nat. Rev. Urol.* **19**, 101–115 (2022).
9. Kumar, A. et al. Substantial interindividual and limited intra-individual genomic diversity among tumors from men with metastatic prostate cancer. *Nat. Med.* **22**, 369–378 (2016).
10. Cancer Genome Atlas Research Network. The molecular taxonomy of primary prostate cancer. *Cell* **163**, 1011–1025 (2015).
11. Tomlins, S. A. et al. Recurrent fusion of TMPRSS2 and ETS transcription factor genes in prostate cancer. *Science* **310**, 644–648 (2005).
12. Clark, J. et al. Complex patterns of ETS gene alteration arise during cancer development in the human prostate. *Oncogene* **27**, 1993–2003 (2008).
13. Clark, J. P. & Cooper, C. S. ETS gene fusions in prostate cancer. *Nat. Rev. Urol.* **6**, 429–439 (2009).
14. Espiritu, S. M. G. et al. The evolutionary landscape of localized prostate cancers drives clinical aggression. *Cell* **173**, 1003–1013.e1015 (2018).
15. Salami, S. S. et al. Transcriptomic heterogeneity in multifocal prostate cancer. *JCI Insight* **3**, e123468 (2018).
16. Falzarano, S. M. et al. ERG rearrangement is present in a subset of transition zone prostatic tumors. *Mod. Pathol.* **23**, 1499–1506 (2010).
17. Varma, M., Shah, R. B., Williamson, S. R. & Berney, D. M. 2019 Gleason grading recommendations from ISUP and GUPS: broadly concordant but with significant differences. *Virchows Arch.* **478**, 813–815 (2021).
18. Rubin, M. A., Girelli, G. & Demichelis, F. Genomic correlates to the newly proposed grading prognostic groups for prostate cancer. *Eur. Urol.* **69**, 557–560 (2016).
19. Wilkinson, S. et al. Nascent prostate cancer heterogeneity drives evolution and resistance to intense hormonal therapy. *Eur. Urol.* **80**, 746–757 (2021).
20. Aggarwal, R. et al. Clinical and genomic characterization of treatment-emergent small-cell neuroendocrine prostate cancer: a multi-institutional prospective study. *J. Clin. Oncol.* **36**, 2492–2503 (2018).
21. Robinson, D. et al. Integrative clinical genomics of advanced prostate cancer. *Cell* **161**, 1215–1228 (2015).
22. Birniewies, M. et al. Understanding the tumor immune microenvironment (TIME) for effective therapy. *Nat. Med.* **24**, 541–550 (2018).
23. Hofbauer, L. C. et al. Novel approaches to target the microenvironment of bone metastasis. *Nat. Rev. Clin. Oncol.* **18**, 488–505 (2021).
24. Garon, E. B. et al. Pembrolizumab for the treatment of non-small-cell lung cancer. *N. Engl. J. Med.* **372**, 2018–2028 (2015).
25. Robert, C. et al. Pembrolizumab versus ipilimumab in advanced melanoma. *N. Engl. J. Med.* **372**, 2521–2532 (2015).
26. Abida, W. et al. Analysis of the prevalence of microsatellite instability in prostate cancer and response to immune checkpoint blockade. *JAMA Oncol.* **5**, 471–478 (2019).
27. van Bokhoven, A. et al. Molecular characterization of human prostate carcinoma cell lines. *Prostate* **57**, 205–225 (2003).
28. Russell, P. J. & Kingsley, E. A. Human prostate cancer cell lines. *Methods Mol. Med.* **81**, 21–39 (2003).
29. van Weerden, W. M., Bangma, C. & de Wit, R. Human xenograft models as useful tools to assess the potential of novel therapeutics in prostate cancer. *Br. J. Cancer* **100**, 13–18 (2009).
30. Namekawa, T., Ikeda, K., Horie-Inoue, K. & Inoue, S. Application of prostate cancer models for preclinical study: advantages and limitations of cell lines, patient-derived xenografts, and three-dimensional culture of patient-derived cells. *Cells* **8**, 74 (2019).
31. Nguyen, H. M. et al. LuCaP prostate cancer patient-derived xenografts reflect the molecular heterogeneity of advanced disease and serve as models for evaluating cancer therapeutics. *Prostate* **77**, 654–671 (2017).
32. Young, S. R. et al. Establishment and serial passage of cell cultures derived from LuCaP xenografts. *Prostate* **73**, 1251–1262 (2013).
33. Stone, K. R., Mickey, D. D., Wunderli, H., Mickey, G. H. & Paulson, D. F. Isolation of a human prostate carcinoma cell line (DU 145). *Int. J. Cancer* **21**, 274–281 (1978).
34. Kaighn, M. E., Narayan, K. S., Ohnuki, Y., Lechner, J. F. & Jones, L. W. Establishment and characterization of a human prostatic carcinoma cell line (PC-3). *Invest. Urol.* **17**, 16–23 (1979).
35. Horoszewicz, J. S. et al. The LNCaP cell line—a new model for studies on human prostatic carcinoma. *Prog. Clin. Biol. Res.* **37**, 115–132 (1980).
36. van Bokhoven, A., Varella-Garcia, M., Korch, C., Hessels, D. & Miller, G. J. Widely used prostate carcinoma cell lines share common origins. *Prostate* **47**, 36–51 (2001).
37. van Bokhoven, A., Varella-Garcia, M., Korch, C. & Miller, G. J. TSU-Pr1 and JCA-1 cells are derivatives of T24 bladder carcinoma cells and are not of prostatic origin. *Cancer Res.* **61**, 6340–6344 (2001).
38. Rubin, M. A. et al. Rapid (“warm”) autopsy study for procurement of metastatic prostate cancer. *Clin. Cancer Res.* **6**, 1038–1045 (2000).
39. Lee, Y. G. et al. Establishment and characterization of a new human prostatic cancer cell line: DuCaP. *Vivo* **15**, 157–162 (2001).
40. Korenchuk, S. et al. VCaP, a cell-based model system of human prostate cancer. *Vivo* **15**, 163–168 (2001).
41. Sfano, K. S. et al. Identification of replication competent murine gammaretroviruses in commonly used prostate cancer cell lines. *PLoS ONE* **6**, e20874 (2011).
42. Griffiths, J. C. The laboratory diagnosis of prostatic adenocarcinoma. *Crit. Rev. Clin. Lab. Sci.* **19**, 187–204 (1983).
43. Moch, H., Humphrey, P. A., Ulbright, T. M. & Reuter, V. *WHO Classification of Tumours of the Urinary System and Male Genital Organs*. (International Agency for Research on Cancer, 2016).
44. Merkens, L. et al. Aggressive variants of prostate cancer: underlying mechanisms of neuroendocrine transdifferentiation. *J. Exp. Clin. Cancer Res.* **41**, 46 (2022).
45. Grossman, H. B., Wedemeyer, G., Ren, L. & Carey, T. E. UM-SCP-1, a new human cell line derived from a prostatic squamous cell carcinoma. *Cancer Res.* **44**, 4111–4117 (1984).
46. Kim, C. J., Kushima, R., Okada, Y. & Seto, A. Establishment and characterization of a prostatic small-cell carcinoma cell line (PSK-1) derived from a patient with Klinefelter syndrome. *Prostate* **42**, 287–294 (2000).
47. Okasho, K. et al. Establishment and characterization of a novel treatment-related neuroendocrine prostate cancer cell line KUCaP13. *Cancer Sci.* **112**, 2781–2791 (2021).
48. Steinelstel, J. et al. Detecting predictive androgen receptor modifications in circulating prostate cancer cells. *Oncotarget* **10**, 4213–4223 (2019).
49. Jividen, K. et al. Genomic analysis of DNA repair genes and androgen signaling in prostate cancer. *BMC Cancer* **18**, 960 (2018).
50. Cornford, P. et al. EAU-EANM-ESTRO-ESUR-SIOG Guidelines on Prostate Cancer. Part II-2020 Update: treatment of relapsing and metastatic prostate cancer. *Eur. Urol.* **79**, 263–282 (2021).
51. Teroerde, M. et al. In Prostate Cancer [internet] (eds Bott, S. R. J. & Ng, K. L.) (Exon Publications, 2021).
52. Perryman, L. A. et al. Over-expression of p53 mutants in LNCaP cells alters tumor growth and angiogenesis in vivo. *Biochem. Biophys. Res. Commun.* **345**, 1207–1214 (2006).
53. Lee, J. K. et al. N-Myc drives neuroendocrine prostate cancer initiated from human prostate epithelial cells. *Cancer Cell* **29**, 536–547 (2016).
54. Souza, A. G. et al. Comparative assay of 2D and 3D cell culture models: proliferation, gene expression and anticancer drug response. *Curr. Pharm. Des.* **24**, 1689–1694 (2018).
55. Sutherland, R. M. Cell and environment interactions in tumor microregions: the multicell spheroid model. *Science* **240**, 177–184 (1988).
56. Dietrichs, D. et al. Three-dimensional growth of prostate cancer cells exposed to simulated microgravity. *Front. Cell Dev. Biol.* **10**, 841017 (2022).
57. Grimm, D. et al. The fight against cancer by microgravity: the multicellular spheroid as a metastasis model. *Int. J. Mol. Sci.* **23**, 3073 (2022).
58. Fontana, F. et al. Three-dimensional cell cultures as an in vitro tool for prostate cancer modeling and drug discovery. *Int. J. Mol. Sci.* **21**, 6806 (2020).
59. Fots, R. A simple hanging drop cell culture protocol for generation of 3D spheroids. *J. Vis. Exp.* <https://doi.org/10.3791/2720> (2011).
60. Hagemann, J. et al. Spheroid-based 3D cell cultures enable personalized therapy testing and drug discovery in head and neck cancer. *Anticancer. Res.* **37**, 2201–2210 (2017).
61. Halfter, K. et al. Prospective cohort study using the breast cancer spheroid model as a predictor for response to neoadjuvant therapy—the SpheroNEO study. *BMC Cancer* **15**, 519 (2015).
62. Bray, L. J., Hutmacher, D. W. & Bock, N. Addressing patient specificity in the engineering of tumor models. *Front. Bioeng. Biotechnol.* **7**, 217 (2019).
63. Gillet, J. P., Varma, S. & Gottesman, M. M. The clinical relevance of cancer cell lines. *J. Natl. Cancer Inst.* **105**, 452–458 (2013).
64. Ingram, M. et al. Tissue engineered tumor models. *Biotech. Histochem.* **85**, 213–229 (2010).
65. Hsiao, A. Y. et al. Microfluidic system for formation of PC-3 prostate cancer co-culture spheroids. *Biomaterials* **30**, 3020–3027 (2009).
66. Bansal, N. et al. BMI-1 Targeting interferes with patient-derived tumor-initiating cell survival and tumor growth in prostate cancer. *Clin. Cancer Res.* **22**, 6176–6191 (2016).
67. Bansal, N. et al. Enrichment of human prostate cancer cells with tumor initiating properties in mouse and zebrafish xenografts by differential adhesion. *Prostate* **74**, 187–200 (2014).
68. Linxweiler, J. et al. Patient-derived, three-dimensional spheroid cultures provide a versatile translational model for the study of organ-confined prostate cancer. *J. Cancer Res. Clin. Oncol.* **145**, 551–559 (2019).
69. Joubert, E., Voissiere, A., Penault-Llorca, F., Cachin, F. & Miot-Noirault, E. Multicellular tumor spheroids of LNCaP-Luc prostate cancer cells as in vitro screening models for cytotoxic drugs. *Am. J. Cancer Res.* **12**, 1116–1128 (2022).
70. Gao, D. et al. Organoid cultures derived from patients with advanced prostate cancer. *Cell* **159**, 176–187 (2014).

Review article

71. Cheaito, K. et al. Establishment and characterization of prostate organoids from treatment-naïve patients with prostate cancer. *Oncol. Lett.* **23**, 6 (2022).
72. Drost, J. et al. Organoid culture systems for prostate epithelial and cancer tissue. *Nat. Protoc.* **11**, 347–358 (2016).
73. Pauli, C. et al. Personalized in vitro and in vivo cancer models to guide precision medicine. *Cancer Discov.* **7**, 462–477 (2017).
74. Kamatar, A., Gunay, G. & Acar, H. Natural and synthetic biomaterials for engineering multicellular tumor spheroids. *Polymers* **12**, 2506 (2020).
75. Van Hemertryk, A. et al. Modeling prostate cancer treatment responses in the organoid era: 3D environment impacts drug testing. *Biomolecules* **11**, 1572 (2021).
76. Fong, E. L. et al. Hydrogel-based 3D model of patient-derived prostate xenograft tumors suitable for drug screening. *Mol. Pharm.* **11**, 2040–2050 (2014).
77. Bray, L. J. et al. Multi-parametric hydrogels support 3D in vitro bioengineered microenvironment models of tumour angiogenesis. *Biomaterials* **53**, 609–620 (2015).
78. Furesi, G., Rauner, M. & Hofbauer, L. C. Emerging players in prostate cancer–bone Niche communication. *Trends Cancer* **7**, 112–121 (2021).
79. Shokohmand, A. et al. Microenvironment engineering of osteoblastic bone metastases reveals osteomimicry of patient-derived prostate cancer xenografts. *Biomaterials* **220**, 119402 (2019).
80. Bock, N. et al. Engineering osteoblastic metastases to delineate the adaptive response of androgen-deprived prostate cancer in the bone metastatic microenvironment. *Bone Res.* **7**, 13 (2019).
81. Bock, N. et al. In vitro engineering of a bone metastases model allows for study of the effects of antiandrogen therapies in advanced prostate cancer. *Sci. Adv.* **7**, eabg2564 (2021).
82. Pereira, B. A. et al. Tissue engineered human prostate microtissues reveal key role of mast cell-derived tryptase in potentiating cancer-associated fibroblast (CAF)-induced morphometric transition in vitro. *Biomaterials* **197**, 72–85 (2019).
83. Merz, L. et al. Tumor tissue slice cultures as a platform for analyzing tissue-penetration and biological activities of nanoparticles. *Eur. J. Pharm. Biopharm.* **112**, 45–50 (2017).
84. Perez, L. M. & Nonn, L. Harnessing the utility of ex vivo patient prostate tissue slice cultures. *Front. Oncol.* **12**, 864723 (2022).
85. Zhao, H. et al. Patient-derived tissue slice grafts accurately depict response of high-risk primary prostate cancer to androgen deprivation therapy. *J. Transl. Med.* **11**, 199 (2013).
86. Figiel, S. et al. Functional organotypic cultures of prostate tissues: a relevant preclinical model that preserves hypoxia sensitivity and calcium signaling. *Am. J. Pathol.* **189**, 1268–1275 (2019).
87. van de Merbel, A. F. et al. An ex vivo tissue culture model for the assessment of individualized drug responses in prostate and bladder cancer. *Front. Oncol.* **8**, 400 (2018).
88. Zhang, W. et al. Ex vivo treatment of prostate tumor tissue recapitulates in vivo therapy response. *Prostate* **79**, 390–402 (2019).
89. Gerlach, M. M. et al. Slice cultures from head and neck squamous cell carcinoma: a novel test system for drug susceptibility and mechanisms of resistance. *Br. J. Cancer* **110**, 479–488 (2014).
90. Koerfer, J. et al. Organotypic slice cultures of human gastric and esophagogastric junction cancer. *Cancer Med.* **5**, 1444–1453 (2016).
91. Sonnichsen, R. et al. Individual susceptibility analysis using patient-derived slice cultures of colorectal carcinoma. *Clin. Colorectal Cancer* **17**, e189–e199 (2018).
92. Merz, F. et al. Organotypic slice cultures of human glioblastoma reveal different susceptibilities to treatments. *Neuro Oncol.* **15**, 670–681 (2013).
93. Chakrabarty, S. et al. A microfluidic cancer-on-chip platform predicts drug response using organotypic tumor slice culture. *Cancer Res.* **82**, 510–520 (2021).
94. Astolfi, M. et al. Micro-dissected tumor tissues on chip: an ex vivo method for drug testing and personalized therapy. *Lab Chip* **16**, 312–325 (2016).
95. Dorrigiv, D. et al. Microdissected tissue vs tissue slices: a comparative study of tumor explant models cultured on-chip and off-chip. *Cancers* **13**, 4208 (2021).
96. Kashaninejad, N. et al. Organ-tumor-on-a-chip for chemosensitivity assay: a critical review. *Micromachines* **7**, 130 (2016).
97. Pandya, H. J. et al. A microfluidic platform for drug screening in a 3D cancer microenvironment. *Biosens. Bioelectron.* **94**, 632–642 (2017).
98. Kunzi-Rapp, K. et al. Chorioallantoic membrane assay: vascularized 3-dimensional cell culture system for human prostate cancer cells as an animal substitute model. *J. Urol.* **166**, 1502–1507 (2001).
99. Wu, X., Gong, S., Roy-Burman, P., Lee, P. & Culig, Z. Current mouse and cell models in prostate cancer research. *Endocr. Relat. Cancer* **20**, R155–R170 (2013).
100. Chung, L. W. et al. Co-inoculation of tumorigenic rat prostate mesenchymal cells with non-tumorigenic epithelial cells results in the development of carcinosarcoma in syngeneic and athymic animals. *Int. J. Cancer* **43**, 1179–1187 (1989).
101. Li, Y. et al. Decrease in stromal androgen receptor associates with androgen-independent disease and promotes prostate cancer cell proliferation and invasion. *J. Cell Mol. Med.* **12**, 2790–2798 (2008).
102. Craig, M., Ying, C. & Loberg, R. D. Co-inoculation of prostate cancer cells with U937 enhances tumor growth and angiogenesis in vivo. *J. Cell Biochem.* **103**, 1–8 (2008).
103. Aigner, A. et al. Ribozyme-targeting of a secreted FGF-binding protein (FGF-BP) inhibits proliferation of prostate cancer cells in vitro and in vivo. *Oncogene* **21**, 5733–5742 (2002).
104. Klink, J. C. et al. Resveratrol worsens survival in SCID mice with prostate cancer xenografts in a cell-line specific manner, through paradoxical effects on oncogenic pathways. *Prostate* **73**, 754–762 (2013).
105. Chen, Q. H. Curcumin-based anti-prostate cancer agents. *Anticancer Agents Med. Chem.* **15**, 138–156 (2015).
106. Jin, X. et al. DUB3 promotes BET inhibitor resistance and cancer progression by deubiquitinating BRD4. *Mol. Cell* **71**, 592–605.e594 (2018).
107. Metzger, E. et al. KMT9 monomethylates histone H4 lysine 12 and controls proliferation of prostate cancer cells. *Nat. Struct. Mol. Biol.* **26**, 361–371 (2019).
108. Vosoglou-Nomikos, T., Pater, J. L. & Seymour, L. Clinical predictive value of the in vitro cell line, human xenograft, and mouse allograft preclinical cancer models. *Clin. Cancer Res.* **9**, 4227–4239 (2003).
109. Yin, Z. et al. Current research developments of patient-derived tumour xenograft models (Review). *Exp. Ther. Med.* **22**, 1206 (2021).
110. Xin, L., Ide, H., Kim, Y., Dubey, P. & Witte, O. N. In vivo regeneration of murine prostate from dissociated cell populations of postnatal epithelia and urogenital sinus mesenchyme. *Proc. Natl. Acad. Sci. USA* **100**, 11896–11903 (2003).
111. Wang, Y. et al. An orthotopic metastatic prostate cancer model in SCID mice via grafting of a transplantable human prostate tumor line. *Lab. Invest.* **85**, 1392–1404 (2005).
112. Liao, C. P., Adisetyo, H., Liang, M. & Roy-Burman, P. Cancer-associated fibroblasts enhance the gland-forming capability of prostate cancer stem cells. *Cancer Res.* **70**, 7294–7303 (2010).
113. Wang, X. et al. A luminal epithelial stem cell that is a cell of origin for prostate cancer. *Nature* **461**, 495–500 (2009).
114. Stephenson, R. A. et al. Metastatic model for human prostate cancer using orthotopic implantation in nude mice. *J. Natl. Cancer Inst.* **84**, 951–957 (1992).
115. Jäger, W. et al. Orthotopic mouse models of urothelial cancer. *Methods Mol. Biol.* **1655**, 177–197 (2018).
116. Singh, A. S. & Figg, W. D. In vivo models of prostate cancer metastasis to bone. *J. Urol.* **174**, 820–826 (2005).
117. Parajuli, K. R., Zhang, Q., Liu, S. & You, Z. Aminomethylphosphonic acid inhibits growth and metastasis of human prostate cancer in an orthotopic xenograft mouse model. *Oncotarget* **7**, 10616–10626 (2016).
118. Hoffman, R. M. Orthotopic metastatic (MetaMouse) models for discovery and development of novel chemotherapy. *Methods Mol. Med.* **111**, 297–322 (2005).
119. Xiang, Y. et al. SPARCL1 suppresses metastasis in prostate cancer. *Mol. Oncol.* **7**, 1019–1030 (2013).
120. Thalmann, G. N. et al. Androgen-independent cancer progression and bone metastasis in the LNCaP model of human prostate cancer. *Cancer Res.* **54**, 2577–2581 (1994).
121. Pettaway, C. A. et al. Selection of highly metastatic variants of different human prostatic carcinomas using orthotopic implantation in nude mice. *Clin. Cancer Res.* **2**, 1627–1636 (1996).
122. Patel, B. J. et al. CL1-GFP: an androgen independent metastatic tumor model for prostate cancer. *J. Urol.* **164**, 1420–1425 (2000).
123. Duan, Z. et al. Th17 cells promote tumor growth in an immunocompetent orthotopic mouse model of prostate cancer. *Am. J. Clin. Exp. Urol.* **7**, 249–261 (2019).
124. Lardizabal, J., Ding, J., Delwar, Z., Rennie, P. S. & Jia, W. A TRAMP-derived orthotopic prostate syngeneic (TOPS) cancer model for investigating anti-tumor treatments. *Prostate* **78**, 457–468 (2018).
125. Anker, J. F., Mok, H., Naseem, A. F., Thumbikat, P. & Abdulkadir, S. A. A bioluminescent and fluorescent orthotopic syngeneic murine model of androgen-dependent and castration-resistant prostate cancer. *J. Vis. Exp.* <https://doi.org/10.3791/57301> (2018).
126. Lange, T. et al. Development and characterization of a spontaneously metastatic patient-derived xenograft model of human prostate cancer. *Sci. Rep.* **8**, 17535 (2018).
127. Shi, M., Wang, Y., Lin, D. & Wang, Y. Patient-derived xenograft models of neuroendocrine prostate cancer. *Cancer Lett.* **525**, 160–169 (2022).
128. Rea, D. et al. Mouse models in prostate cancer translational research: from xenograft to PDX. *Biomod. Res. Int.* **2016**, 9750795 (2016).
129. van Weerden, W. M. et al. Development of seven new human prostate tumor xenograft models and their histopathological characterization. *Am. J. Pathol.* **149**, 1055–1062 (1996).
130. Palanisamy, N. et al. The MD Anderson prostate cancer patient-derived xenograft series (MDA PCa PDX) captures the molecular landscape of prostate cancer and facilitates marker-driven therapy development. *Clin. Cancer Res.* **26**, 4933–4946 (2020).
131. Risbridger, G. P. et al. The MURAL collection of prostate cancer patient-derived xenografts enables discovery through preclinical models of uro-oncology. *Nat. Commun.* **12**, 5049 (2021).
132. Evrard, Y. A. et al. Systematic establishment of robustness and standards in patient-derived xenograft experiments and analysis. *Cancer Res.* **80**, 2286–2297 (2020).
133. Lin, D. et al. High fidelity patient-derived xenografts for accelerating prostate cancer discovery and drug development. *Cancer Res.* **74**, 1272–1283 (2014).
134. Marques, R. B. et al. High efficacy of combination therapy using PI3K/AKT inhibitors with androgen deprivation in prostate cancer preclinical models. *Eur. Urol.* **67**, 1177–1185 (2015).
135. Varkaris, A. et al. Integrating murine and clinical trials with cabozantinib to understand roles of MET and VEGFR2 as targets for growth inhibition of prostate cancer. *Clin. Cancer Res.* **22**, 107–121 (2016).
136. Hammer, S. et al. Preclinical efficacy of a PSMA-targeted thorium-227 conjugate (PSMA-TTC), a targeted alpha therapy for prostate cancer. *Clin. Cancer Res.* **26**, 1985–1996 (2020).
137. Ben-David, U. et al. Patient-derived xenografts undergo mouse-specific tumor evolution. *Nat. Genet.* **49**, 1567–1575 (2017).
138. Woo, X. Y. et al. Conservation of copy number profiles during engraftment and passaging of patient-derived cancer xenografts. *Nat. Genet.* **53**, 86–99 (2021).

Review article

139. Verma, B., Ritchie, M. & Mancini, M. Development and applications of patient-derived xenograft models in humanized mice for oncology and immune-oncology drug discovery. *Curr. Protoc. Pharmacol.* **78**, 14.41.11–14.41.12 (2017).
140. Shultz, L. D., Brehm, M. A., Garcia-Martinez, J. V. & Greiner, D. L. Humanized mice for immune system investigation: progress, promise and challenges. *Nat. Rev. Immunol.* **12**, 786–798 (2012).
141. Roth, M. D. & Harui, A. Human tumor infiltrating lymphocytes cooperatively regulate prostate tumor growth in a humanized mouse model. *J. Immunother. Cancer* **3**, 12 (2015).
142. Valta, M. et al. Critical evaluation of the subcutaneous engraftments of hormone naïve primary prostate cancer. *Transl. Androl. Urol.* **9**, 1120–1134 (2020).
143. Liu, G. et al. Perturbation of NK cell peripheral homeostasis accelerates prostate carcinoma metastasis. *J. Clin. Invest.* **123**, 4410–4422 (2013).
144. Alix-Panabières, C. & Pantel, K. Liquid biopsy: from discovery to clinical application. *Cancer Discov.* **11**, 858–873 (2021).
145. Faugeroux, V. et al. Genetic characterization of a unique neuroendocrine transdifferentiation prostate circulating tumor cell-derived eXplant model. *Nat. Commun.* **11**, 1884 (2020).
146. Keller, L. & Pantel, K. Unravelling tumour heterogeneity by single-cell profiling of circulating tumour cells. *Nat. Rev. Cancer* **19**, 553–567 (2019).
147. Mout, L. et al. Generating human prostate cancer organoids from leukapheresis enriched circulating tumour cells. *Eur. J. Cancer* **150**, 179–189 (2021).
148. Gunti, S., Hoke, A. T. K., Vu, K. P. & London, N. R. Jr Organoid and spheroid tumor models: techniques and applications. *Cancers* **13**, 874 (2021).
149. Köcher, S. et al. A functional ex vivo assay to detect PARP1-EJ repair and radiosensitization by PARP-inhibitor in prostate cancer. *Int. J. Cancer* **144**, 1685–1696 (2019).
150. Greenberg, N. M. et al. Prostate cancer in a transgenic mouse. *Proc. Natl Acad. Sci. USA* **92**, 3439–3443 (1995).
151. Ellwood-Yen, K. et al. Myc-driven murine prostate cancer shares molecular features with human prostate tumors. *Cancer Cell* **4**, 223–238 (2003).
152. Freeman, K. W. et al. Inducible prostate intraepithelial neoplasia with reversible hyperplasia in conditional FGFR1-expressing mice. *Cancer Res.* **63**, 8256–8263 (2003).
153. Hurwitz, A. A., Foster, B. A., Allison, J. P., Greenberg, N. M. & Kwon, E. D. The TRAMP mouse as a model for prostate cancer. *Curr. Protoc. Immunol.* <https://doi.org/10.1002/0471142735.im2005s45> (2001).
154. Alajati, A. et al. CDCP1 overexpression drives prostate cancer progression and can be targeted in vivo. *J. Clin. Invest.* **130**, 2435–2450 (2020).
155. Jin, R. J. et al. The nuclear factor- κ B pathway controls the progression of prostate cancer to androgen-independent growth. *Cancer Res.* **68**, 6762–6769 (2008).
156. Wu, X. et al. Generation of a prostate epithelial cell-specific Cre transgenic mouse model for tissue-specific gene ablation. *Mech. Dev.* **101**, 61–69 (2001).
157. Kim, M. J. et al. Cooperativity of Nkx3.1 and Pten loss of function in a mouse model of prostate carcinogenesis. *Proc. Natl Acad. Sci. USA* **99**, 2884–2889 (2002).
158. Wang, S. et al. Prostate-specific deletion of the murine Pten tumor suppressor gene leads to metastatic prostate cancer. *Cancer Cell* **4**, 209–221 (2003).
159. Mulholland, D. J. et al. Cell autonomous role of PTEN in regulating castration-resistant prostate cancer growth. *Cancer Cell* **19**, 792–804 (2011).
160. Blattner, M. et al. SPOP mutation drives prostate tumorigenesis in vivo through coordinate regulation of PI3K/mTOR and AR signaling. *Cancer Cell* **31**, 436–451 (2017).
161. Ding, Z. et al. Telomerase reactivation following telomere dysfunction yields murine prostate tumors with bone metastases. *Cell* **148**, 896–907 (2012).
162. Mulholland, D. J. et al. Pten loss and RAS/MAPK activation cooperate to promote EMT and metastasis initiated from prostate cancer stem/progenitor cells. *Cancer Res.* **72**, 1878–1889 (2012).
163. Dardenne, E. et al. N-Myc induces an EZH2-mediated transcriptional program driving neuroendocrine prostate cancer. *Cancer Cell* **30**, 563–577 (2016).
164. Ding, Z. et al. SMAD4-dependent barrier constrains prostate cancer growth and metastatic progression. *Nature* **470**, 269–273 (2011).
165. Zhao, D. et al. Chromatin regulator CHD1 remodels the immunosuppressive tumor microenvironment in PTEN-deficient prostate cancer. *Cancer Discov.* **10**, 1374–1387 (2020).
166. Lu, X. et al. Effective combinatorial immunotherapy for castration-resistant prostate cancer. *Nature* **543**, 728–732 (2017).
167. Taavitsainen, S. et al. Single-cell ATAC and RNA sequencing reveal pre-existing and persistent cells associated with prostate cancer relapse. *Nat. Commun.* **12**, 5307 (2021).
168. Brady, L. et al. Inter- and intra-tumor heterogeneity of metastatic prostate cancer determined by digital spatial gene expression profiling. *Nat. Commun.* **12**, 1426 (2021).
169. Zhao, T. et al. Spatial genomics enables multi-modal study of clonal heterogeneity in tissues. *Nature* **601**, 85–91 (2022).
170. Chelebian, E. et al. Morphological features extracted by AI associated with spatial transcriptomics in prostate cancer. *Cancers* **13**, 4837 (2021).
171. Haffner, M. C. et al. Genomic and phenotypic heterogeneity in prostate cancer. *Nat. Rev. Urol.* **18**, 79–92 (2021).
172. Hong, M. K. et al. Tracking the origins and drivers of subclonal metastatic expansion in prostate cancer. *Nat. Commun.* **6**, 6605 (2015).
173. Gundem, G. et al. The evolutionary history of lethal metastatic prostate cancer. *Nature* **520**, 353–357 (2015).
174. van de Wetering, M. et al. Prospective derivation of a living organoid biobank of colorectal cancer patients. *Cell* **161**, 933–945 (2015).
175. Cao, J., Chan, W. C. & Chow, M. S. S. Use of conditional reprogramming cell, patient derived xenograft and organoid for drug screening for individualized prostate cancer therapy: current and future perspectives (Review). *Int. J. Oncol.* **60**, 52 (2022).
176. Heidegger, I. et al. Comprehensive characterization of the prostate tumor microenvironment identifies CXCR4/CXCL12 crosstalk as a novel antiangiogenic therapeutic target in prostate cancer. *Mol. Cancer* **21**, 132 (2022).
177. Zhang, Z. et al. Tumor microenvironment-derived NRG1 promotes antiandrogen resistance in prostate cancer. *Cancer Cell* **38**, 279–296.e279 (2020).
178. Javier-DesLoges, J. et al. The microbiome and prostate cancer. *Prostate Cancer Prostatic Dis.* **25**, 159–174 (2021).
179. Poore, G. D. et al. Microbiome analyses of blood and tissues suggest cancer diagnostic approach. *Nature* **579**, 567–574 (2020).
180. Daisley, B. A. et al. Abiraterone acetate preferentially enriches for the gut commensal *Akkermansia muciniphila* in castrate-resistant prostate cancer patients. *Nat. Commun.* **11**, 4822 (2020).
181. Pernigoni, N. et al. Commensal bacteria promote endocrine resistance in prostate cancer through androgen biosynthesis. *Science* **374**, 216–224 (2021).
182. Terrisse, S. et al. Immune system and intestinal microbiota determine efficacy of androgen deprivation therapy against prostate cancer. *J. Immunother. Cancer* **10**, e004191 (2022).
183. Meijer, T. G., Naipal, K. A., Jager, A. & van Gent, D. C. Ex vivo tumor culture systems for functional drug testing and therapy response prediction. *Future Sci. OA* **3**, FSO190 (2017).
184. Contreras-Trujillo, H. et al. Deciphering intratumoral heterogeneity using integrated clonal tracking and single-cell transcriptome analyses. *Nat. Commun.* **12**, 6522 (2021).
185. von Amsberg, G. et al. Immunotherapy in advanced prostate cancer-light at the end of the tunnel? *Int. J. Mol. Sci.* **23**, 2569 (2022).
186. Goldenberg, S. L., Nir, G. & Salcudean, S. E. A new era: artificial intelligence and machine learning in prostate cancer. *Nat. Rev. Urol.* **16**, 391–403 (2019).
187. Kann, B. H., Hosny, A. & Aerts, H. Artificial intelligence for clinical oncology. *Cancer Cell* **39**, 916–927 (2021).
188. Gupta, R. et al. Artificial intelligence to deep learning: machine intelligence approach for drug discovery. *Mol. Divers.* **25**, 1315–1360 (2021).
189. Mickey, D. D., Stone, K. R., Stone, M. P. & Paulson, D. F. Morphologic and immunologic studies of human prostatic carcinoma. *Cancer Treat. Rep.* **61**, 133–138 (1977).
190. Williams, R. D. et al. Biochemical markers of cultured human prostatic epithelium. *J. Urol.* **119**, 768–771 (1978).
191. Williams, R. D. Human urologic cancer cell lines. *Invest. Urol.* **17**, 359–363 (1980).
192. Horoszewicz, J. S. et al. LNCaP model of human prostatic carcinoma. *Cancer Res.* **43**, 1809–1818 (1983).
193. Claas, F. H. & van Steenbrugge, G. J. Expression of HLA-like structures on a permanent human tumor line PC-93. *Tissue Antigens* **21**, 227–232 (1983).
194. Romijn, J. C., Verkoelen, C. F. & Schroeder, F. H. Application of the MTT assay to human prostate cancer cell lines in vitro: establishment of test conditions and assessment of hormone-stimulated growth and drug-induced cytostatic and cytotoxic effects. *Prostate* **12**, 99–110 (1988).
195. Carney, D. N. et al. Establishment and identification of small cell lung cancer cell lines having classic and variant features. *Cancer Res.* **45**, 2913–2923 (1985).
196. Johnson, B. E. et al. Retention of chromosome 3 in extrapulmonary small cell cancer shown by molecular and cytogenetic studies. *J. Natl. Cancer Inst.* **81**, 1223–1228 (1989).
197. Gingrich, J. R. et al. Establishment and characterization of a new human prostatic carcinoma cell line (DuPro-1). *J. Urol.* **146**, 915–919 (1991).
198. Plymate, S. R. et al. Effects of sex hormone binding globulin (SHBG) on human prostatic carcinoma. *J. Steroid Biochem. Mol. Biol.* **40**, 833–839 (1991).
199. Mehta, P. P. et al. Gap-junctional communication in normal and neoplastic prostate epithelial cells and its regulation by cAMP. *Mol. Carcinog.* **15**, 18–32 (1996).
200. Marques, R. B. et al. Androgen receptor modifications in prostate cancer cells upon long-term androgen ablation and antiandrogen treatment. *Int. J. Cancer* **117**, 221–229 (2005).
201. Zhai, H. Y. et al. Androgen-repressed phenotype in human prostate cancer. *Proc. Natl. Acad. Sci. USA* **93**, 15152–15157 (1996).
202. Klein, K. A. et al. Progression of metastatic human prostate cancer to androgen independence in immunodeficient SCID mice. *Nat. Med.* **3**, 402–408 (1997).
203. Navone, N. M. et al. Establishment of two human prostate cancer cell lines derived from a single bone metastasis. *Clin. Cancer Res.* **3**, 2493–2500 (1997).
204. Navone, N. M. et al. TabBO: a model reflecting common molecular features of androgen-independent prostate cancer. *Clin. Cancer Res.* **6**, 1190–1197 (2000).
205. Pretlow, T. G. et al. Xenografts of primary human prostatic carcinoma. *J. Natl. Cancer Inst.* **85**, 394–398 (1993).
206. Wainstein, M. A. et al. CWR22: androgen-dependent xenograft model derived from a primary human prostatic carcinoma. *Cancer Res.* **54**, 6049–6052 (1994).
207. Sramkoski, R. M. et al. A new human prostate carcinoma cell line, 22Rv1. *Vitr. Cell Dev. Biol. Anim.* **35**, 403–409 (1999).
208. Gregory, C. W., Johnson, R. T. Jr, Mohler, J. L., French, F. S. & Wilson, E. M. Androgen receptor stabilization in recurrent prostate cancer is associated with hypersensitivity to low androgen. *Cancer Res.* **61**, 2892–2898 (2001).
209. Wu, H. C. et al. Derivation of androgen-independent human LNCaP prostatic cancer cell sublines: role of bone stromal cells. *Int. J. Cancer* **57**, 406–412 (1994).
210. Loop, S. M., Rozanski, T. A. & Ostenson, R. C. Human primary prostate tumor cell line, ALVA-31: a new model for studying the hormonal regulation of prostate tumor cell growth. *Prostate* **22**, 93–108 (1993).
211. Nakhlia, A. M. & Rosner, W. Characterization of ALVA-41 cells, a new human prostatic cancer cell line. *Steroids* **59**, 586–589 (1994).

Review article

212. Brothman, A. R., Lesho, L. J., Somers, K. D., Wright, G. L. Jr & Merchant, D. J. Phenotypic and cytogenetic characterization of a cell line derived from primary prostatic carcinoma. *Int. J. Cancer* **44**, 898–903 (1989).
213. Bae, V. L., Jackson-Cook, C. K., Brothman, A. R., Maygarden, S. J. & Ware, J. L. Tumorigenicity of SV40 T antigen immortalized human prostate epithelial cells: association with decreased epidermal growth factor receptor (EGFR) expression. *Int. J. Cancer* **58**, 721–729 (1994).
214. Bello, D., Webber, M. M., Kleinman, H. K., Wartinger, D. D. & Rhim, J. S. Androgen responsive adult human prostatic epithelial cell lines immortalized by human papillomavirus 18. *Carcinogenesis* **18**, 1215–1223 (1997).
215. Rhim, J. S. et al. Stepwise immortalization and transformation of adult human prostate epithelial cells by a combination of HPV-18 and v-Ki-ras. *Proc. Natl Acad. Sci. USA* **91**, 11874–11878 (1994).
216. Webber, M. M. et al. Prostate specific antigen and androgen receptor induction and characterization of an immortalized adult human prostatic epithelial cell line. *Carcinogenesis* **17**, 1641–1646 (1996).
217. Webber, M. M. et al. A human prostatic stromal myofibroblast cell line WPMY-1: a model for stromal–epithelial interactions in prostatic neoplasia. *Carcinogenesis* **20**, 1185–1192 (1999).
218. Koochekpour, S. et al. Establishment and characterization of a primary androgen-responsive African-American prostate cancer cell line, E006AA. *Prostate* **60**, 141–152 (2004).
219. Ke, X. S. et al. Epithelial to mesenchymal transition of a primary prostate cell line with switches of cell adhesion modules but without malignant transformation. *PLoS ONE* **3**, e3368 (2008).
220. Theodore, S. et al. Establishment and characterization of a pair of non-malignant and malignant tumor derived cell lines from an African American prostate cancer patient. *Int. J. Oncol.* **37**, 1477–1482 (2010).
221. Szczyrba, J. et al. The microRNA profile of prostate carcinoma obtained by deep sequencing. *Mol. Cancer Res.* **8**, 529–538 (2010).
222. Acevedo, V. D. et al. Inducible FGFR-1 activation leads to irreversible prostate adenocarcinoma and an epithelial-to-mesenchymal transition. *Cancer Cell* **12**, 559–571 (2007).
223. Bhatia-Gaur, R. et al. Roles for Nkx3.1 in prostate development and cancer. *Genes Dev.* **13**, 966–977 (1999).
224. Wan, X. et al. Prostate cancer cell-stromal cell crosstalk via FGFR1 mediates antitumor activity of dovitinib in bone metastases. *Sci. Transl. Med.* **6**, 252ra122 (2014).
225. Pecqueux, C. et al. FGF-2 is a driving force for chromosomal instability and a stromal factor associated with adverse clinico-pathological features in prostate cancer. *Urol. Oncol.* **36**, 365.e315–365.e326 (2018).
226. Wach, S. et al. MicroRNA profiles of prostate carcinoma detected by multiplatform microRNA screening. *Int. J. Cancer* **130**, 611–621 (2012).
227. Wach, S. et al. Exploring the MIR143-UPAR axis for the inhibition of human prostate cancer cells in vitro and in vivo. *Mol. Ther. Nucleic Acids* **16**, 272–283 (2019).
228. McClurg, U. L. et al. Human ex vivo prostate tissue model system identifies ING3 as an oncogene. *Br. J. Cancer* **118**, 713–726 (2018).
229. Ewe, A. et al. Optimized polyethylenimine (PEI)-based nanoparticles for siRNA delivery, analyzed in vitro and in an ex vivo tumor tissue slice culture model. *Drug Deliv. Transl. Res.* **7**, 206–216 (2017).
230. Karimov, M., Appelhans, D., Ewe, A. & Aigner, A. The combined disulfide cross-linking and tyrosine-modification of very low molecular weight linear PEI synergistically enhances transfection efficacies and improves biocompatibility. *Eur. J. Pharm. Biopharm.* **161**, 56–65 (2021).
231. Hu, R. et al. Ligand-independent androgen receptor variants derived from splicing of cryptic exons signify hormone-refractory prostate cancer. *Cancer Res.* **69**, 16–22 (2009).
232. Antonarakis, E. S. et al. AR-V7 and resistance to enzalutamide and abiraterone in prostate cancer. *N. Engl. J. Med.* **371**, 1028–1038 (2014).
233. Scher, H. I. et al. Association of AR-V7 on circulating tumor cells as a treatment-specific biomarker with outcomes and survival in castration-resistant prostate cancer. *JAMA Oncol.* **2**, 1441–1449 (2016).
234. Armstrong, A. J. et al. Prospective multicenter validation of androgen receptor splice variant 7 and hormone therapy resistance in high-risk castration-resistant prostate cancer: the PROPHET study. *J. Clin. Oncol.* **37**, 1120–1129 (2019).
235. Bernemann, C. et al. Expression of AR-V7 in circulating tumour cells does not preclude response to next generation androgen deprivation therapy in patients with castration resistant prostate cancer. *Eur. Urol.* **71**, 1–3 (2017).
236. Bernemann, C., Krabbe, L. M. & Schrader, A. J. Considerations for AR-V7 testing in clinical routine practice. *Ann. Transl. Med.* **7**, S378 (2019).
237. Del Re, M. et al. The detection of androgen receptor splice variant 7 in plasma-derived exosomal RNA strongly predicts resistance to hormonal therapy in metastatic prostate cancer patients. *Eur. Urol.* **71**, 680–687 (2017).
238. Del Re, M. et al. Androgen receptor gain in circulating free DNA and splicing variant 7 in exosomes predict clinical outcome in CRPC patients treated with abiraterone and enzalutamide. *Prostate Cancer Prostatic Dis.* **24**, 524–531 (2021).
239. Lieb, V. et al. Cell-free DNA variant sequencing using plasma and AR-V7 testing of circulating tumor cells in prostate cancer patients. *Cells* **10**, 3223 (2021).
240. Li, Q. et al. Clinicopathological characteristics of androgen receptor splicing variant 7 (AR-V7) expression in patients with castration resistant prostate cancer: a systematic review and meta-analysis. *Transl. Oncol.* **14**, 101145 (2021).
241. Brown, L. C., Lu, C., Antonarakis, E. S., Luo, J. & Armstrong, A. J. Androgen receptor variant-driven prostate cancer II: advances in clinical investigation. *Prostate Cancer Prostatic Dis.* **23**, 367–380 (2020).

Acknowledgements

The authors' own research related to the topics of this article was supported by the Deutsche Forschungsgemeinschaft (DFG; AI 24/26-1 (A.A.), TA 145/17-1 (H.T.), WE 5844/5-1 (St.W.), SPP2048 'microbone' SA 3254/1-1 (V.S.), SPP2048 'microbone' (Project-ID 401179983; S.P.), Ki 672/6-1 (J.K.), SPP 'microbone' and ERC Advanced Investigator Grant INJURMET (No. 834974; K.P.) as well as SFB 992 (Project-ID 403222702), SFB 1381 (Project-ID 89986987), SFB 850 and Schu688/15-1 to R.S.). The work was further supported by a grant of the Rudolf Becker-Foundation (T0321/36080/2020/kg) to S.P. and J.K., by the Federal Ministry for Economic Affairs and Climate Action (S.D.), by a fellowship of the University of Lübeck and by a Gerok fellowship within the SPP 2084 to S.P.

Author contributions

All authors researched data for the article, made substantial contributions to discussion of content, and wrote the manuscript. A.A. reviewed and edited the manuscript before submission.

Competing interests

The authors declare no competing interests.

Additional information

Supplementary information The online version contains supplementary material available at <https://doi.org/10.1038/s41585-022-00677-z>.

Correspondence should be addressed to Achim Aigner.

Peer review information *Nature Reviews Urology* thanks Johannes Linxweiler, Marco De Velasco and the other, anonymous, reviewer(s) for their contribution to the peer review of this work.

Reprints and permissions information is available at www.nature.com/reprints.

Publisher's note Springer Nature remains neutral with regard to jurisdictional claims in published maps and institutional affiliations.

Springer Nature or its licensor (e.g. a society or other partner) holds exclusive rights to this article under a publishing agreement with the author(s) or other rightsholder(s); author self-archiving of the accepted manuscript version of this article is solely governed by the terms of such publishing agreement and applicable law.

© Springer Nature Limited 2022